

SU(3) analysis of four-quark operators: $K \rightarrow \pi\pi$ and vacuum matrix elements

A. Pich¹⁾ and A. Rodríguez-Sánchez²⁾

¹⁾ Departament de Física Teòrica, IFIC, CSIC — Universitat de València
Edifici d'Instituts de Paterna, Apt. Correus 22085, E-46071 València, Spain

²⁾ Université Paris-Saclay, CNRS/IN2P3, IJCLab, 91405 Orsay, France

Abstract

Hadronic matrix elements of local four-quark operators play a central role in non-leptonic kaon decays, while vacuum matrix elements involving the same kind of operators appear in inclusive dispersion relations, such as those relevant in τ -decay analyses. Using an $SU(3)_L \otimes SU(3)_R$ decomposition of the operators, we derive generic relations between these matrix elements, extending well-known results that link observables in the two different sectors. Two relevant phenomenological applications are presented. First, we determine the electroweak-penguin contribution to the kaon CP-violating ratio ε'/ε , using the measured hadronic spectral functions in τ decay. Second, we fit our $SU(3)$ dynamical parameters to the most recent lattice data on $K \rightarrow \pi\pi$ matrix elements. The comparison of this numerical fit with results from previous analytical approaches provides an interesting anatomy of the $\Delta I = \frac{1}{2}$ enhancement, confirming old suggestions about its underlying dynamical origin.

1 Introduction

Local operators with dimension larger than four, such as four-quark operators, play a key role in quantitatively understanding the low-energy dynamics of renormalizable theories. When working with a quantum field theory involving widely-separated scales, such as the Standard Model (SM), the logarithms of large scale ratios induce higher-order corrections that slow-down, if not directly spoil, the standard perturbative series. The use of short-distance techniques like the Operator Product Expansion (OPE) [1] to separate scales and Renormalization Group Equations (RGE) to resum those logarithmic corrections becomes then a must [2–5]. When these techniques are applied, the resulting Effective Field Theory (EFT) contains a series of low-energy operators, whose quantitative role in a given observable is, in general, inversely proportional to their dimensions.

At low energies, the short-distance logarithmic resummation is not enough. Owing to confinement and the associated growing of the strong coupling, the low-energy theory cannot be formulated in terms of approximately-free quarks and gluons; the relevant degrees of freedom are, instead, hadrons. In practice, one runs perturbatively the EFT to energies as small as possible, so that all large short-distance logarithms can be reabsorbed into the computed Wilson coefficients, but the hadronic matrix elements of their associated operators must still be determined with non-perturbative methods.

At very low energies, the only observed hadrons are pions, kaons and eta bosons. Due to their flavour structure, non-leptonic kaon decays cannot occur through strong or electromagnetic interactions; one needs to trace back their origin to the only source of flavour-breaking in the SM, the W boson, whose imprint in the effective low-energy Lagrangian appears through dimension-six four-quark operators. The non-perturbative calculation of the corresponding hadronic matrix elements is a formidable task and current theoretical uncertainties for the associated observables are unfortunately large [6]. Improved lattice computations, *e.g.*, see [7], may change the situation in the future.

A more precise knowledge arises in inclusive semileptonic processes involving three light quark flavours, such as hadronic tau decays or electron-positron annihilation into hadrons [8]. Although they have a quite different nature, the former being a weak-interaction transition and the latter an electromagnetic one, their associated hadronic distributions can be studied with the same theoretical formalism, since rigorous dispersion relations [9, 10] connect them with two-point correlation functions of quark currents, leading to very precise predictions [11]. It is precisely in the OPE of these two-point correlation functions [12] where the four-quark operators appear. In the same way that local quark operators can give non-zero matrix elements in transitions among hadrons, they can also acquire non-vanishing expectation values in the non-perturbative QCD vacuum. A well-known example is the $\bar{q}q$ condensate that plays a key role in the dynamical breaking of chiral symmetry. Unlike in non-leptonic kaon decays, the numerical role of four-quark operators is very small in the τ decay width because they enter suppressed by six powers of the tau mass. Nevertheless, with the achieved experimental accuracy, it is possible to extract significant dynamical information on some operators from the current τ data

samples.

Non-trivial relations among matrix elements involving different four-quark operators can be derived, using their known symmetry transformations together with our knowledge of strong interactions at low energies. Many of these relations have been exploited in the past, but they appear somehow scattered in the literature [13–31]. In the following, we aim to provide a self-contained derivation, based only on symmetry considerations and EFT, and apply them to the phenomenology of non-leptonic kaon decays. As an important application, we will determine the electromagnetic-penguin contribution to ε'/ε , using the measured hadronic spectral functions in τ decay. Our determination will be compared with the updated values obtained combining Chiral Perturbation Theory (χ PT) and large- N_C techniques [32, 33], and with the most recent lattice results [7].

We will also present a global fit to the available lattice data on $K \rightarrow \pi\pi$ matrix elements [7, 34, 35], in terms of a complete set of independent dynamical parameters with well-defined $SU(3)_L \otimes SU(3)_R$ transformation properties, at next-to-leading order (NLO) in α_s (short-distance logarithms) and χ PT. The comparison of this numerical fit with previous analytical results makes possible to achieve a quantitative assessment of the different approximations adopted in those approaches. This provides an interesting anatomy of the $\Delta I = \frac{1}{2}$ enhancement, confirming old suggestions about its underlying dynamical origin.

The paper is organized as follows. Section 2 focuses on the derivation of symmetry relations, making use of effective Lagrangians. The formalism is applied to strangeness-changing transitions in Section 3, which recovers the usual notation employed in χ PT [6]. In Section 4, we apply the same tools to analyze the four-quark vacuum condensates appearing in the correlation functions of the QCD currents. This provides the wanted connection between the two sectors, making possible to determine with τ data a non-perturbative dynamical parameter characterizing the electroweak-penguin operator Q_8 . This determination is presented in Section 5, after introducing all necessary dispersive tools. A phenomenological analysis of $K \rightarrow \pi\pi$ matrix elements is presented in Section 6, which contains the implications of our dispersive result for ε'/ε and the numerical fit to the most recent lattice data. A detailed discussion of our current understanding of the $\Delta I = \frac{1}{2}$ rule is given there, based on the fitted results and the previous analytical knowledge. As a final consistency check, we also provide a precise determination of the pion decay constant, combining the parameters fitted to the lattice data with the measured inclusive distribution of the final hadrons in τ decay. The main results of our paper are finally summarized in Section 7.

2 Low-energy realization of four-quark operators

The massless QCD Lagrangian with three quark flavours,

$$\mathcal{L}_{\text{QCD}}^0 = -\frac{1}{4} G_{\mu\nu}^a G_a^{\mu\nu} + i \bar{q}_L \gamma^\mu D_\mu q_L + i \bar{q}_R \gamma^\mu D_\mu q_R \quad (1)$$

with $q^T = (u, d, s)$, is invariant under $(L, R) \in SU(3)_L \otimes SU(3)_R$ global transformations in the flavour space: $q'_{L,i} = L_i^j q_{L,j}$, $q'_{R,i} = R_i^j q_{R,j}$, where $q_L = \frac{1}{2}(1 - \gamma_5)q$ and $q_R = \frac{1}{2}(1 + \gamma_5)q$ denote the left and right quark chiralities. This chiral symmetry is however not seen in the hadronic spectrum, which is only invariant under $SU(3)_V$ transformations with $L = R$. Thus, chiral symmetry is dynamically broken by the QCD vacuum, giving rise to eight 0^- massless Goldstone bosons that can be identified with the lightest pseudoscalar octet (π , K , η).

Together with parity (P) and charge-conjugation (C) invariance, chiral symmetry enforces very strong constraints on the low-energy dynamics of these (pseudo)Goldstone bosons that can be most easily analyzed with an effective Lagrangian expanded in powers of derivatives [36]. A convenient parametrization of the Goldstone fields is provided by the unitary matrix $U[\phi_i] = e^{i\lambda_i\phi_i/F}$, transforming as $U \rightarrow RUL^\dagger$ under chiral rotations. At leading order (LO) in the derivative expansion, the effective Goldstone Lagrangian contains only two terms [37]:

$$\mathcal{L}_{\text{eff}} = \frac{F^2}{4} \text{Tr}(D_\mu U^\dagger D^\mu U + U^\dagger \chi + \chi^\dagger U) + \mathcal{O}(p^4). \quad (2)$$

The covariant derivative $D^\mu U = \partial^\mu U - ir^\mu U + iU\ell^\mu$ includes auxiliary external left (ℓ^μ) and right (r^μ) matrix-valued vector sources coupled to the quarks, which allow us to easily derive the low-energy realization of the QCD currents [36]. The second term incorporates the couplings to external scalar (s) and pseudoscalar (p) sources through $\chi = 2B_0(s + ip)$. Taking $p = 0$ and $s = \mathcal{M} = \text{diag}(m_u, m_d, m_s)$, this term implements the explicit breaking of chiral symmetry induced by the non-zero quark masses, generating the physical masses of the eight pseudoscalar bosons. The LO effective Lagrangian \mathcal{L}_{eff} completely determines the $\mathcal{O}(p^2)$ contributions to the Goldstone masses and scattering amplitudes, in terms of the quark masses, and the two low-energy couplings (LECs) F and B_0 , which are related to the pion decay constant and the $\bar{q}q$ vacuum condensate [38].

The underlying QCD Lagrangian, including the external sources ℓ^μ , r^μ , s and p , and its low-energy Chiral Perturbation Theory (χ PT) [37, 39] realization \mathcal{L}_{eff} are connected through the path integral expression

$$\begin{aligned} \exp\{iZ[\ell^\mu, r^\mu, s, p]\} &= \int \mathcal{D}q \mathcal{D}\bar{q} \mathcal{D}G_\mu \exp\left\{i \int d^4x \mathcal{L}_{\text{QCD}}\right\} \\ &= \int \mathcal{D}U \exp\left\{i \int d^4x \mathcal{L}_{\text{eff}}\right\}. \end{aligned} \quad (3)$$

By taking functional derivatives with respect to the appropriate external sources in both terms of the equality, one finds the explicit low-energy expressions of the QCD quark currents. This dictionary will be exploited below to derive some useful relations among four-quark operators. Many of those symmetry relations are well-known, although quite often they are presented without a crystal-clear derivation or resorting to soft-pion methods. The next subsections compile them together, using a much simpler approach purely based on symmetry arguments.

2.1 Chiral symmetry decomposition

At low energies below the electroweak scale v , the renormalizable SM gives rise to an effective short-distance Lagrangian that contains dimension-six four-fermion operators. They originate from integrating out the heavy degrees of freedom (t , H , Z , W^\pm , b , c), which is needed in order to resum the large perturbative logarithms generated by the sizeable ratios of mass scales [2–5]. The phenomenological effects of these ‘irrelevant’ electroweak operators are suppressed by a factor $E^2/v^2 \sim G_F E^2$, where E is the energy scale of the process. They can then be treated as small perturbations to the QCD Lagrangian, in the sense that it is usually enough to analyze their implications to LO in G_F .

Let us then consider the extended QCD Lagrangian

$$\mathcal{L} = \mathcal{L}_{\text{QCD}}^{N_f=3} + [t_L]_{ik}^{jl} (\bar{q}_L^i \gamma^\mu q_{Lj}) (\bar{q}_L^k \gamma_\mu q_{Ll}) + [t_R]_{ik}^{jl} (\bar{q}_R^i \gamma^\mu q_{Rj}) (\bar{q}_R^k \gamma_\mu q_{Rl}), \quad (4)$$

with auxiliary tensorial sources $[t_{L,R}]_{ik}^{jl}$. These sources will be later identified with the corresponding Wilson coefficients of the short-distance electroweak Lagrangian, which are obviously scale and scheme dependent because the four-quark operators need to be properly renormalized.

Taking into account the transformation of the quark currents under P and C ,

$$(\bar{q}_{L(R)}^i \gamma^\mu q_{L(R)j}) \xrightarrow{P} (\bar{q}_{R(L)}^i \gamma_\mu q_{R(L)j}), \quad (\bar{q}_{L(R)}^i \gamma^\mu q_{L(R)j}) \xrightarrow{C} -(\bar{q}_{R(L)}^j \gamma^\mu q_{R(L)i}), \quad (5)$$

invariance under P and C is recovered if

$$[t_{L(R)}]_{ik}^{jl} \xrightarrow{P} [t_{R(L)}]_{ik}^{jl}, \quad [t_{L(R)}]_{ik}^{jl} \xrightarrow{C} [t_{R(L)}]_{jl}^{ik}. \quad (6)$$

Moreover, under chiral flavour transformations

$$[t_{L(R)}]_{ik}^{jl} \rightarrow L(R)_{j'}^\dagger{}^j L(R)_{l'}^\dagger{}^l t_{i'k'}^{j'l'} L(R)_i{}^{i'} L(R)_k{}^{k'}, \quad (7)$$

in order to preserve the chiral invariance of \mathcal{L} . Imposing this formal symmetry on the external sources (spurions), one can easily work out the symmetry implications for the different types of four-fermion operators.

It is convenient to identify those combinations of four-quark operators belonging to irreducible representations of the chiral group. The transformation (7) corresponds to the 81-dimensional representation $(\bar{3} \otimes 3) \otimes (\bar{3} \otimes 3)$ of $SU(3)_{L(R)}$, which can be decomposed into irreducible symmetric/antisymmetric representations with dimensions¹ 1, 8, 10 and 27. This decomposition can be done in a straightforward way, taking into account that the $SU(3)$ transformations preserve traces and the symmetry under exchange of upper ($j \leftrightarrow l$) and/or lower ($i \leftrightarrow k$) indices.²

¹The representation r stands here for $(1_L, r_R)$ or $(r_L, 1_R)$, corresponding to $[t_R]$ and $[t_L]$, respectively.

²A pair of upper or lower indices give 6 symmetric plus 3 antisymmetric possibilities ($3 \otimes 3 = 6 \oplus 3$). Considering the single and double traces of an upper and a lower index, the 36 symmetric-symmetric (SS) configurations can be decomposed in 27 ($= 36 - 9$) fully traceless ones, plus other 8 ($= 36 - 27 - 1$) configurations with non-vanishing single traces but null double trace, plus the singlet combination where both traces are non-zero [40]. Obviously, the 9 antisymmetric-antisymmetric (AA) configurations can only produce the octet plus singlet possibilities. A singlet combination cannot be present in the AS or SA configurations, which are then decomposed into $10 \oplus 8$.

Defining a tensor scalar product as

$$\mathcal{A} \cdot \mathcal{B} = A_{kl}^{ij} B_{ij}^{kl}, \quad (8)$$

one can define an orthonormal basis in terms of irreducible subsets:

$$\{e_{27S}^a, e_{8S}^{aS}, e_{1S}^S, e_{10S}^a, e_{8S}^{aA}, e_{10A}^a, e_{8A}^{aS}, e_{8A}^{aA}, e_{1A}^A\}, \quad (9)$$

where S and A refer to the symmetric or antisymmetric character of the representation with respect to the upper or lower indices. One can then write any tensor in this basis as

$$\mathcal{A} = \mathcal{A}_{rN}^{aM} e_{rN}^{aM}, \quad (10)$$

where the coefficient is, using orthonormality,

$$\mathcal{A}_{rN}^{aM} = \mathcal{A} \cdot e_{rN}^{aM} = A_{kl}^{ij} [e_{rN}^{aM}]_{ij}^{kl}. \quad (11)$$

Since the operators in Eq. (4) are symmetric under the simultaneous exchange $(i, k) \leftrightarrow (j, l)$, we only need to consider the symmetric-symmetric ($1 \oplus 8 \oplus 27$) and antisymmetric-antisymmetric ($1 \oplus 8$) configurations. The fully-symmetric singlet and octet basis elements take the form:

$$[e_{1S}^S]_{ik}^{jl} = \frac{1}{\sqrt{24}} (\delta_i^j \delta_k^l + \delta_i^l \delta_k^j), \quad (12)$$

$$[e_{8S}^S]_{ik}^{jl} = \frac{1}{\sqrt{40}} (\lambda_i^{a,j} \delta_k^l + \lambda_i^{a,l} \delta_k^j + \lambda_k^{a,j} \delta_i^l + \lambda_k^{a,l} \delta_i^j), \quad (13)$$

with $\lambda_i^{a,j}$ any basis of traceless $SU(3)$ matrices such that $\text{Tr}(\lambda^a \lambda^b) = 2\delta^{ab}$, for which we adopt the conventional Gell-Mann choice. Instead of building an explicit basis of 27 symmetric tensors, it is simpler to subtract the singlet and octet pieces from the symmetric-symmetric component of the tensor:

$$\mathcal{A}_{27S}^S = \mathcal{A}_S^S - (\mathcal{A}_S^S \cdot e_{1S}^S) e_{1S}^S - (\mathcal{A}_S^S \cdot e_{8S}^S) e_{8S}^S. \quad (14)$$

The remaining antisymmetric-antisymmetric pieces can be projected in a fully analogous way with the corresponding basis elements

$$[e_{1A}^A]_{ik}^{jl} = \frac{1}{\sqrt{12}} (\delta_i^j \delta_k^l - \delta_i^l \delta_k^j), \quad (15)$$

$$[e_{8A}^A]_{ik}^{jl} = \frac{1}{\sqrt{8}} (\lambda_i^{a,j} \delta_k^l - \lambda_i^{a,l} \delta_k^j - \lambda_k^{a,j} \delta_i^l + \lambda_k^{a,l} \delta_i^j). \quad (16)$$

2.2 Effective χ PT operators

To build the corresponding structures in the low-energy χ PT framework, one just needs to combine the transformation properties in Eqs. (6) and (7) with those of the basic chiral building blocks. Under P and C [41],

$$(D_{\mu_1} \cdots D_{\mu_n} U)_i^j \xrightarrow{P} (D^{\mu_1} \cdots D^{\mu_n} U)_i^{\dagger j}, \quad \chi_i^j \xrightarrow{P} \chi_i^{\dagger j}, \quad (17)$$

$$(D_{\mu_1} \cdots D_{\mu_n} U)_i^j \xrightarrow{C} (D_{\mu_1} \cdots D_{\mu_n} U)_j^i, \quad \chi_i^j \xrightarrow{C} \chi_j^i, \quad (18)$$

and under flavour,³

$$(D_{\mu_1} \cdots D_{\mu_n} U)_i^j \rightarrow R_i^{i'} (D_{\mu_1} \cdots D_{\mu_n} U)_{i'}^{j'} L_j^{\dagger j'}, \quad \chi_i^j \rightarrow R_i^{i'} \chi_{i'}^{j'} L_j^{\dagger j'}. \quad (19)$$

It turns useful to define simple χ PT structures transforming as pure left or right objects:

$$L_\mu \equiv i U^\dagger D_\mu U \rightarrow L L_\mu L^\dagger, \quad U^\dagger \chi \rightarrow L U^\dagger \chi L^\dagger, \quad (20)$$

$$R_\mu \equiv i U (D_\mu U)^\dagger \rightarrow R R_\mu R^\dagger, \quad U \chi^\dagger \rightarrow R U \chi^\dagger R^\dagger. \quad (21)$$

The LO building block compatible with a non-zero 27-plet arises at $\mathcal{O}(p^2)$ from connecting $L_{\mu_k}^i L_l^{\mu_j}$ to $[t_L]_{ij}^{kl}$ and $R_{\mu_k}^i R_l^{\mu_j}$ to $[t_R]_{ij}^{kl}$. Making use of the relation (14) to project the 27 piece, and requiring invariance under the discrete symmetries P and C , one finds:

$$\begin{aligned} \mathcal{L}_{27} = a_{27} \frac{F^4}{8} & \left\{ [t_L]_{ik}^{jl} \left([L_j^{\mu,i} L_{\mu,l}^k + L_j^{\mu,k} L_{\mu,l}^i] - \frac{1}{12} \text{Tr}(L_\mu L^\mu) [\delta_j^i \delta_l^k + \delta_l^i \delta_j^k] \right. \right. \\ & \left. \left. - \frac{1}{10} \text{Tr}(\lambda^a L_\mu L^\mu) [\lambda_{a,j}^i \delta_l^k + \lambda_{a,l}^i \delta_j^k + \lambda_{a,j}^k \delta_l^i + \lambda_{a,l}^k \delta_j^i] + \mathcal{O}(p^4) \right) \right. \\ & \left. + L \leftrightarrow R \right\}. \quad (22) \end{aligned}$$

Parity invariance requires the result to be symmetric under the exchange $L \leftrightarrow R$. Therefore, the $(27_L, 1_R)$ and $(1_L, 27_R)$ components share the same normalization. Symmetries alone do not allow to fix the (μ dependent) global constant a_{27} , which encodes details on the non-perturbative QCD dynamics. We have normalized it with a factor F^4 so that a_{27} is a dimensionless quantity. Notice that there are no other independent colour or spinor structures that can give a 27-plet made out of four-quark operators.⁴ At this chiral order, our non-perturbative ignorance for the 27-plet part of any (SM or beyond SM) effective four-quark operator is encoded in a single constant.

³Schematically, for building blocks purposes one may just represent them as $t_{LL}^{LL}, U_R^L, \chi_R^L, U_L^{\dagger R}, \chi_L^{\dagger R}, t_{RR}^{RR}$.

⁴For $(V \pm A) \times (V \pm A)$ operators, Fierz transformations trivially relate the two possible colour-singlet structures.

Projecting with the fully-symmetric octet basis element in Eq. (13), one directly finds the effective symmetric octet Lagrangian:⁵

$$\mathcal{L}_8^S = a_8^S \frac{F^4}{80} \left\{ [t_L]_{ik}^{jl} \text{Tr}(\lambda^a L_\mu L^\mu) + [t_R]_{ik}^{jl} \text{Tr}(\lambda^a R_\mu R^\mu) \right\} (\lambda_{a,j}^i \delta_l^k + \lambda_{a,l}^i \delta_j^k + \lambda_{a,j}^k \delta_l^i + \lambda_{a,l}^k \delta_j^i) + \mathcal{O}(p^4). \quad (23)$$

A completely analogous derivation leads to the antisymmetric octet one:

$$\mathcal{L}_8^A = -a_8^A \frac{F^4}{16} \left\{ [t_L]_{ik}^{jl} \text{Tr}(\lambda^a L_\mu L^\mu) + [t_R]_{ik}^{jl} \text{Tr}(\lambda^a R_\mu R^\mu) \right\} (\lambda_{a,j}^i \delta_l^k - \lambda_{a,l}^i \delta_j^k - \lambda_{a,j}^k \delta_l^i + \lambda_{a,l}^k \delta_j^i) + \mathcal{O}(p^4). \quad (24)$$

The parameters a_{27} , a_8^S and a_8^A depend on the short-distance renormalization scale μ . Since there is only a 27-plet structure, the μ dependence encoded in $a_{27}(\mu)$ cancels exactly the one carried by the $[t_L]$ and $[t_R]$ tensorial sources in Eq. (22). The cancellation of renormalization-scale dependences is more subtle in the octet sector because the QCD interaction mixes different flavour-octet structures.

With only symmetry consideration, no useful information can be derived from the singlet structures, since there are pure $\mathcal{O}(p^0)$ contact terms, such as $[t_{L(R)}]_{ij}^{ij}$ and $[t_{L(R)}]_{ji}^{ij}$, that are not related to the Goldstone dynamics.

2.3 Left-right four-quark operators

Let us now consider the Lagrangian

$$\mathcal{L} = \mathcal{L}_{\text{QCD}}^{N_f=3} + [t_{LR}^{\delta\delta}]_{ik}^{jl} (\bar{q}_L^i \gamma^\mu q_{Lj}) (\bar{q}_R^k \gamma_\mu q_{Rl}) + [t_{LR}^{\lambda\lambda}]_{ik}^{jl} (\bar{q}_L^i \gamma^\mu T^a q_{Lj}) (\bar{q}_R^k \gamma_\mu T^a q_{Rl}), \quad (25)$$

where $T^a = \frac{1}{2} \lambda_C^a$ are the generators of the colour $SU(3)_C$ group with λ_C^a the corresponding Gell-Mann matrices in colour space. Both $t_{LR}^{\delta\delta}$ and $t_{LR}^{\lambda\lambda}$ share the same symmetry transformations. We will omit the superscript when we refer to any of them. The Lagrangian is invariant under discrete symmetries provided that

$$[t_{LR}]_{ik}^{jl} \xrightarrow{P} [t_{LR}]_{ki}^{lj}, \quad [t_{LR}]_{ik}^{jl} \xrightarrow{C} [t_{LR}]_{lj}^{ki}, \quad (26)$$

while invariance under chiral flavour transformations requires

$$[t_{LR}]_{ik}^{jl} \rightarrow L_{j'}^\dagger{}^j R_{l'}^\dagger{}^l [t_{LR}]_{i'k'}^{j'l'} L_i{}^{i'} R_k{}^{k'}. \quad (27)$$

The decomposition into irreducible representations is now simpler because each fermion bilinear transforms with a different $SU(3)$ group. Thus, we have the $\bar{3} \otimes 3 = 1 \oplus 8$

⁵An additional allowed octet structure is obtained, replacing $\text{Tr}(\lambda^a L_\mu L^\mu)$ and $\text{Tr}(\lambda^a R_\mu R^\mu)$ in Eq. (23) by $\text{Tr}[\lambda^a (U^\dagger \chi + \chi^\dagger U)]$ and $\text{Tr}[\lambda^a (U \chi^\dagger + \chi U^\dagger)]$, respectively [16]. However, it induces a vacuum misalignment through Goldstone tadpoles. Once the Goldstone fields are properly redefined, this $\mathcal{O}(p^2)$ weak mass term is rotated away. Thus, it does not contribute to any physical amplitude [19, 42].

decomposition in each chiral sector, which results in four possible structures transforming as $(1_L, 1_R)$, $(8_L, 1_R)$, $(1_L, 8_R)$, and $(8_L, 8_R)$. Following the same procedure explained before, an associated orthonormal basis is trivially given by

$$[e_{1_L, 1_R}]_{ik}^{jl} = \frac{1}{3} \delta_i^j \delta_k^l, \quad [e_{8_L, 1_R}^a]_{ik}^{jl} = \frac{1}{\sqrt{6}} \lambda_{L,i}^{a,j} \delta_k^l, \quad [e_{1_L, 8_R}^a]_{ik}^{jl} = \frac{1}{\sqrt{6}} \delta_i^j \lambda_{R,k}^{a,l}, \quad [e_{8_L, 8_R}^{ab}]_{ik}^{jl} = \frac{1}{2} \lambda_{L,i}^{a,j} \lambda_{R,k}^{b,l}, \quad (28)$$

where we have made explicit the left or right nature of the different Gell-Mann matrices.

The LO χ PT structure compatible with a nonzero $(8_L, 8_R)$ piece is the $\mathcal{O}(p^0)$ tensor $U_i^{\dagger l} U_k^j$. Projecting it with the corresponding element of the orthonormal basis in Eq. (28), one finds

$$\mathcal{L}_{8_L, 8_R} = \frac{F^6}{4} \left(a_{88}^{\delta\delta} [t_{LR}^{\delta\delta}]_{ik}^{jl} + a_{88}^{\lambda\lambda} [t_{LR}^{\lambda\lambda}]_{ik}^{jl} \right) \lambda_{L,j}^{a,i} \lambda_{R,l}^{b,k} \text{Tr}(\lambda_L^a U^\dagger \lambda_R^b U) + \mathcal{O}(p^2). \quad (29)$$

It can be easily checked that this Lagrangian is invariant under parity and charge conjugation, provided that the external sources transform as indicated in Eq. (26). These two discrete transformations connect the $(8_L, 1_R)$ and $(1_L, 8_R)$ sectors; their corresponding LO effective Lagrangian is easily found to be

$$\mathcal{L}_8^{LR} = \frac{F^4}{6} \left(a_{LR}^{\delta\delta} [t_{LR}^{\delta\delta}]_{ik}^{jl} + a_{LR}^{\lambda\lambda} [t_{LR}^{\lambda\lambda}]_{ik}^{jl} \right) \left\{ \text{Tr}(\lambda_L^a L_\mu L^\mu) \lambda_{L,j}^{a,i} \delta_l^k + \text{Tr}(\lambda_R^a R_\mu R^\mu) \delta_j^i \lambda_{R,l}^{a,k} \right\} + \mathcal{O}(p^4). \quad (30)$$

The global factors F^6 and F^4 have been introduced in order to have dimensionless couplings $a_{88}^{\delta\delta}$, $a_{88}^{\lambda\lambda}$, $a_{LR}^{\delta\delta}$ and $a_{LR}^{\lambda\lambda}$. Once again, the low-energy realization of the remaining singlet structure does not give any useful information.

2.4 Large- N_C limit

At LO in the momentum expansion, all non-trivial dynamical information about the non-singlet flavour structures is then encoded in the seven couplings $a_i(\mu)$. Their expected size can be easily estimated in the limit of a large number of QCD colours N_C , where the colour-singlet currents factorize. The LO χ PT realizations of the left and right QCD currents are just given by [38]

$$(\bar{q}_L^i \gamma^\mu q_{Lj}) \doteq -\frac{1}{2} F^2 L_j^{\mu,i}, \quad (\bar{q}_R^i \gamma^\mu q_{Rj}) \doteq -\frac{1}{2} F^2 R_j^{\mu,i}. \quad (31)$$

This explains the chosen normalization factor in Eq. (22), from which the global factors in (23) and (24) follow. Therefore, the dynamical couplings associated with left-left and right-right four-quark operators take the large- N_C values:

$$a_{27}^\infty(\mu) = 1, \quad a_8^{S,\infty}(\mu) = 1, \quad a_8^{A,\infty}(\mu) = 1. \quad (32)$$

The left-right colour-singlet structure in Eq. (25) does not contribute to the LO χ PT Lagrangians (29) and (30) when $N_C \rightarrow \infty$:

$$a_{88}^{\delta\delta,\infty}(\mu) = 0, \quad a_{LR}^{\delta\delta,\infty}(\mu) = 0. \quad (33)$$

Making a Fierz rearrangement, the colour-octet term can be written as a product of right and left scalar currents:

$$\begin{aligned} (\bar{q}_L^i \gamma^\mu T^a q_{Lj}) (\bar{q}_R^k \gamma_\mu T^a q_{Rl}) &= -(\bar{q}_L^i q_{Rl}) (\bar{q}_R^k q_{Lj}) + \frac{1}{N_C} (\bar{q}_L^{\alpha i} q_{Rl}^\beta) (\bar{q}_R^{\beta k} q_{Lj}^\alpha) \\ &\doteq -B_0^2 F^2 \left\{ \frac{1}{4} F^2 U_i^i U_j^{\dagger k} \right. \\ &\quad + U_i^i [L_5 U^\dagger D_\nu U D^\nu U^\dagger + 2L_7 U^\dagger \text{Tr}(U^\dagger \chi - \chi^\dagger U) + 2L_8 U^\dagger \chi U^\dagger + H_2 \chi^\dagger]_j^k \\ &\quad + [L_5 U D_\nu U^\dagger D^\nu U - 2L_7 U \text{Tr}(U^\dagger \chi - \chi^\dagger U) + 2L_8 U \chi^\dagger U + H_2 \chi]_i^i U_j^{\dagger k} \left. \right\}, \\ &\quad + \mathcal{O}(p^4 N_C^2, p^2 N_C), \end{aligned} \quad (34)$$

where the indices α and β in the first line denote the quark colours (colour-singlet currents are understood whenever colour labels are not explicit). In the last expression we have only kept the large- N_C contributions, using the known χ PT realization of these currents [32]. This fixes the normalization of $a_{88}^{\lambda\lambda}$ and $a_{LR}^{\lambda\lambda}$ in the limit $N_C \rightarrow \infty$:

$$a_{88}^{\lambda\lambda,\infty}(\mu) = -\frac{1}{4} B(\mu), \quad a_{LR}^{\lambda\lambda,\infty}(\mu) = -2 L_5 B(\mu), \quad (35)$$

where the μ -dependent factor

$$B(\mu) \equiv \frac{B_0^2}{F^2} = \left[\frac{M_K^2}{(m_s + m_d)(\mu) F_\pi} \right]^2 \left\{ 1 + \frac{8M_\pi^2}{F_\pi^2} L_5 - \frac{16M_K^2}{F_\pi^2} (2L_8 - L_5) \right\} \quad (36)$$

is related to the quark condensate in the chiral limit, $\langle 0 | \bar{u}u | 0 \rangle = -F^2 B_0$. The constants L_i and H_2 are low-energy couplings of the $\mathcal{O}(p^4)$ χ PT Lagrangian [38].

Thus, $F^2 a_{88}^{\lambda\lambda}(\mu)$ and $a_{LR}^{\lambda\lambda}(\mu)$ are of $\mathcal{O}(N_C^0)$, while $a_{88}^{\delta\delta}(\mu)$ and $a_{LR}^{\delta\delta}(\mu)$ are suppressed by a factor $1/N_C$. The dependence on the renormalization scale of $a_{27}(\mu)$, $a_8^S(\mu)$ and $a_8^A(\mu)$ is also colour suppressed, while the factor $B(\mu)$ captures the exact μ dependence of $a_{88}^{\lambda\lambda,\infty}(\mu)$ and $a_{LR}^{\lambda\lambda,\infty}(\mu)$ in the large- N_C limit. The anomalous dimensions of the left-left and right-right operators are necessarily of NLO in $1/N_C$ because the vector and axial-vector currents are not renormalized. On the other side, the scalar and pseudoscalar QCD currents do depend on renormalization conventions. Only renormalization-invariant combinations such as $m_q \bar{q}^i q_j$ can appear in observable quantities, which explains why the μ dependence of left-right operators scales with the factor $B(\mu) \sim m_q(\mu)^{-2}$ at large- N_C .

3 Strangeness-changing weak transitions

Let us particularize now the previous discussion to the $\Delta S = 1$ and $\Delta S = 2$ transitions. After integrating out the heavy mass scales, the effective $\Delta S = 1$ SM Lagrangian takes

	$z_i(1 \text{ GeV})$	$y_i(1 \text{ GeV})$
1	-0.482	0
2	1.260	0
3	0.00105	0.0307
4	-0.0296	-0.0563
5	0.00699	0.00105
6	-0.0293	-0.103
7	0.0000745	-0.000314
8	0.0000832	0.00115
9	0.000117	-0.0114
10	-0.0000503	0.00475

Table 1: $\Delta S = 1$ Wilson Coefficients at NLO in the $\overline{\text{MS}}$ (NDR) scheme at $\mu = 1 \text{ GeV}$.

the form

$$\mathcal{L}^{\Delta S=1} = G \sum_{i=1}^{10} C_i(\mu) Q_i(\mu), \quad (37)$$

where

$$G \equiv -\frac{G_F}{\sqrt{2}} V_{ud} V_{us}^*, \quad (38)$$

contains the Fermi coupling and the leading quark-mixing parameters, and the sum extends over the standard basis of ten four-quark operators Q_i [2, 43]:

$$\begin{aligned}
Q_1 &= 4 (\bar{s}_L^\alpha \gamma^\mu u_L^\beta) (\bar{u}_L^\beta \gamma_\mu d_L^\alpha), & Q_2 &= 4 (\bar{s}_L \gamma^\mu u_L) (\bar{u}_L \gamma_\mu d_L), \\
Q_3 &= 4 (\bar{s}_L \gamma^\mu d_L) \sum_{q=u,d,s} (\bar{q}_L \gamma_\mu q_L), & Q_4 &= 4 (\bar{s}_L^\alpha \gamma^\mu d_L^\beta) \sum_{q=u,d,s} (\bar{q}_L^\beta \gamma_\mu q_L^\alpha), \\
Q_5 &= 4 (\bar{s}_L \gamma^\mu d_L) \sum_{q=u,d,s} (\bar{q}_R \gamma_\mu q_R), & Q_6 &= 4 (\bar{s}_L^\alpha \gamma^\mu d_L^\beta) \sum_{q=u,d,s} (\bar{q}_R^\beta \gamma_\mu q_R^\alpha), \\
Q_7 &= 6 (\bar{s}_L \gamma^\mu d_L) \sum_{q=u,d,s} e_q (\bar{q}_R \gamma_\mu q_R), & Q_8 &= 6 (\bar{s}_L^\alpha \gamma^\mu d_L^\beta) \sum_{q=u,d,s} e_q (\bar{q}_R^\beta \gamma_\mu q_R^\alpha), \\
Q_9 &= 6 (\bar{s}_L \gamma^\mu d_L) \sum_{q=u,d,s} e_q (\bar{q}_L \gamma_\mu q_L), & Q_{10} &= 6 (\bar{s}_L^\alpha \gamma^\mu d_L^\beta) \sum_{q=u,d,s} e_q (\bar{q}_L^\beta \gamma_\mu q_L^\alpha), \quad (39)
\end{aligned}$$

where α, β are colour indices. The factors e_q denote the corresponding quark charges in units of $e = \sqrt{4\pi\alpha}$. All short-distance dynamical information on the heavy scales is encoded in the Wilson Coefficients $C_i(\mu) = z_i(\mu) + \tau y_i(\mu)$, where $\tau = -\lambda_t/\lambda_u$ with $\lambda_q = V_{qs}^* V_{qd}$. These coefficients can be computed with standard perturbative tools and their numerical values at NLO are given in Table 1.

The effective realization of $\mathcal{L}^{\Delta S=1}$ in the low-energy Goldstone theory is well known [6].

At LO is characterized by three different χ PT structures [16–20, 44–46],

$$\mathcal{L}_{\text{eff}}^{\Delta S=1} = GF^4 \left\{ g_{27} \left(L_2^{\mu 3} L_{\mu 1}^1 + \frac{2}{3} L_2^{\mu 1} L_{\mu 1}^3 \right) + g_8 \text{Tr}(\lambda L^\mu L_\mu) + e^2 g_8 g_{\text{ewk}} F^2 \text{Tr}(\lambda U^\dagger Q U) \right\}, \quad (40)$$

transforming as $(27_L, 1_R)$, $(8_L, 1_R)$ and $(8_L, 8_R)$, respectively. Here, $\lambda \equiv \frac{1}{2}(\lambda_6 - i\lambda_7)$ projects onto the $\bar{s} \rightarrow \bar{d}$ transition and $Q = \frac{1}{3} \text{diag}(2, -1, -1)$ is the quark charge matrix.

Particularizing the tensor sources in Eqs. (4) and (25) to the SM $\Delta S = 1$ Lagrangian (37) and projecting over the different chiral-symmetry components, using Eqs. (22), (23), (24), (29) and (30), one easily finds the expression of the three low-energy couplings in terms of the SM Wilson coefficients:⁶

$$g_{27} = \frac{3}{5} a_{27}(\mu) \left(C_1 + C_2 + \frac{3}{2} C_9 + \frac{3}{2} C_{10} \right) (\mu), \quad (41)$$

$$\begin{aligned} g_8 &= \frac{1}{10} a_8^S(\mu) (C_1 + C_2 + 5C_3 + 5C_4 - C_9 - C_{10})(\mu) \\ &\quad - \frac{1}{2} a_8^A(\mu) (C_1 - C_2 + C_3 - C_4 + C_9 - C_{10})(\mu) \\ &\quad + 4 a_{LR}^{\delta\delta}(\mu) \left(C_5 + \frac{C_6}{N_c} \right) (\mu) + 8 a_{LR}^{\lambda\lambda}(\mu) C_6(\mu), \end{aligned} \quad (42)$$

$$e^2 g_8 g_{\text{ewk}} = 6 \left\{ a_{88}^{\delta\delta}(\mu) \left(C_7 + \frac{C_8}{N_c} \right) (\mu) + 2 a_{88}^{\lambda\lambda}(\mu) C_8(\mu) \right\}. \quad (43)$$

Since the chiral couplings g_{27} , g_8 and g_{ewk} are independent of the short-distance renormalization scale μ , these equations contain also information on the μ dependence of the non-perturbative parameters $a_i(\mu)$. Inserting the large- N_C values of the $a_i(\mu)$ couplings in Eqs. (32), (33) and (35), one recovers the known expressions for the weak χ PT LECs in the limit of a large number of QCD colours [48]:

$$\begin{aligned} g_{27}^\infty &= \frac{3}{5} \left(C_1 + C_2 + \frac{3}{2} C_9 + \frac{3}{2} C_{10} \right), \\ g_8^\infty &= -\frac{2}{5} C_1 + \frac{3}{5} C_2 + C_4 - 16 L_5 B(\mu) C_6(\mu) - \frac{3}{5} C_9 + \frac{2}{5} C_{10}, \\ (e^2 g_8 g_{\text{ewk}})^\infty &= -3 B(\mu) C_8(\mu). \end{aligned} \quad (44)$$

C_6 and C_8 are the only Wilson coefficients carrying an explicit dependence on μ at $N_C \rightarrow \infty$. This dependence is exactly cancelled by the factor $B(\mu)$.

⁶The operator basis is redundant because $Q_4 = -Q_1 + Q_2 + Q_3$, $Q_9 = \frac{3}{2} Q_1 - \frac{1}{2} Q_3$ and $Q_{10} = \frac{1}{2} Q_1 + Q_2 - \frac{1}{2} Q_3$. Thus, Q_4 , Q_9 and Q_{10} can be eliminated redefining appropriately the Wilson coefficients to $C'_1 = C_1 - C_4 + \frac{3}{2} C_9 + \frac{1}{2} C_{10}$, $C'_2 = C_2 + C_4 + C_{10}$ and $C'_3 = C_3 + C_4 - \frac{1}{2} C_9 - \frac{1}{2} C_{10}$. The Fierz transformation needed to rewrite Q_4 in the colour-singlet form of Eq. (4) generates an additional tiny contribution from evanescent operators in the NDR scheme (this correction is zero with the 't Hooft-Veltman prescription for γ_5) [47]. It can be easily incorporated in Eq. (42) with the changes: $C_6 \rightarrow C_6 - \frac{\alpha_s}{4\pi} C_4$, $C_4 \rightarrow C_4 - \frac{\alpha_s}{4\pi} C_4$, $C_3 \rightarrow C_3 + \frac{\alpha_s}{12\pi} C_4$ and $C_5 \rightarrow C_5 + \frac{\alpha_s}{12\pi} C_4$.

3.1 $\Delta S = 2$ Lagrangian

In the SM the mixing between the neutral kaon and its antiparticle is mediated by box diagrams with two W exchanges. In the three-flavour theory, they generate a $\Delta S = 2$ effective Lagrangian that contains one single dimension-six operator [49]:

$$\mathcal{L}^{\Delta S=2} = -\frac{G_F^2 M_W^2}{(4\pi)^2} \mathcal{F}(V_{\text{CKM}}, m_c, m_t) C_{\Delta S=2}(\mu) Q_{\Delta S=2}(\mu), \quad (45)$$

where

$$Q_{\Delta S=2} = 4 (\bar{s}_L \gamma_\mu d_L) (\bar{s}_L \gamma^\mu d_L), \quad (46)$$

$$C_{\Delta S=2}(\mu) = \alpha_s(\mu)^{-2/9} \left[1 + \frac{\alpha_s(\mu)}{4\pi} J_3 \right] \quad (47)$$

and the short-distance factor [50]

$$\mathcal{F}(V_{\text{CKM}}, m_c, m_t) = \lambda_u^2 \eta_{cc} \mathcal{S}(x_c) + \lambda_t^2 \eta_{tt} \mathcal{S}(x_t) + 2\lambda_u \lambda_t \eta_{ut} \mathcal{S}(x_c, x_t) \quad (48)$$

contains the information on the relevant quark-mixing factors λ_q and the heavy mass scales, through the modified Inami-Lim functions $\mathcal{S}(x_q)$ and $\mathcal{S}(x_c, x_t)$, where $x_q = m_q^2/M_W^2$. In the $\overline{\text{MS}}$ scheme, the QCD corrections take the values $J_3 = 1.895$, $\eta_{cc} = 1.87 \pm 0.76$, $\eta_{tt} = 0.5765 \pm 0.0065$ and $\eta_{ut} = 0.402 \pm 0.005$ [50–54].

The corresponding external source tensor in Eq. (4), $[t_L]_{33}^{22}$, belongs to the $(27_L, 1_R)$ multiplet. Using Eq. (22), one finds the effective χ PT realization of this $\Delta S = 2$ operator:

$$\mathcal{L}_{27}^{\Delta S=2} = \frac{G_F^2 M_W^2}{(4\pi)^2} \mathcal{F}(V_{\text{CKM}}, m_c, m_t) g_{\Delta S=2} F^4 L_2^{\mu,3} L_{\mu,2}^3 + \mathcal{O}(p^4), \quad (49)$$

with

$$g_{\Delta S=2} = a_{27}(\mu) C_{\Delta S=2}(\mu). \quad (50)$$

Thus, $a_{27}(\mu)$ depends on the renormalization scale in precisely the opposite way than Eq. (47), so that the product $g_{\Delta S=2}$ remains scale invariant.

Since both involve the same non-perturbative parameter $a_{27}(\mu)$, the chiral couplings $g_{\Delta S=2}$ and g_{27} are directly related through the identity

$$g_{27} = \frac{3}{5} \frac{\left(C_1 + C_2 + \frac{3}{2} C_9 + \frac{3}{2} C_{10} \right)(\mu)}{C_{\Delta S=2}(\mu)} g_{\Delta S=2}. \quad (51)$$

This symmetry relation guarantees that the running of the Wilson coefficients in the numerator matches exactly the one of $C_{\Delta S=2}(\mu)$ in the denominator, so that the ratio is scale invariant. From the measured $K \rightarrow \pi\pi$ rates, one obtains at NLO in χ PT [6, 33]

$$g_{27} = 0.29 \pm 0.02, \quad (52)$$

which implies

$$g_{\Delta S=2} = 0.79 \pm 0.05, \quad (53)$$

and

$$a_{27}(\mu_0) = 0.622 \pm 0.043 \quad (54)$$

at $\mu_0 = 1$ GeV.

The relation between these two 27-plet couplings is usually expressed [13] in terms of the so-called B_K parameter, defined through

$$\langle \bar{K}^0 | Q_{\Delta S=2} | K^0 \rangle = \frac{16}{3} F_K^2 M_K^2 B_K, \quad (55)$$

or the scale-invariant quantity $\hat{B}_K \equiv B_K(\mu) C_{\Delta S=2}(\mu)$. Evaluating this hadronic matrix element with the effective Lagrangian (49), one gets

$$F_K^2 \hat{B}_K = \frac{3}{4} F^2 g_{\Delta S=2} + \mathcal{O}(p^4). \quad (56)$$

Thus, $\frac{3}{4} g_{\Delta S=2}$ and $\frac{3}{4} a_{27}(\mu)$ correspond to the values of \hat{B}_K and $B_K(\mu)$, respectively, in the chiral limit.⁷ Using Eq. (32), one recovers the well-known result $B_K^\infty = \frac{3}{4}$ at large N_C .

The value of $g_{\Delta S=2}$ extracted above from the $K \rightarrow \pi\pi$ rates implies $\hat{B}_K = 0.59 \pm 0.02$ in the chiral limit. This can be compared with the results from explicit calculations with different methods:

$$\lim_{m_q \rightarrow 0} \hat{B}_K = \begin{cases} 0.33 \pm 0.09 & [15] \\ 0.38 \pm 0.15 & [55, 56] \\ 0.36 \pm 0.15 & [30, 57] \end{cases}. \quad (57)$$

Conversely, taking the chiral-limit value of \hat{B}_K from the most recent calculation of Ref. [55], one predicts:

$$g_{\Delta S=2} = 0.51 \pm 0.20, \quad g_{27} = 0.19 \pm 0.07, \quad (58)$$

and

$$a_{27}(\mu_0) = 0.40 \pm 0.16, \quad (59)$$

at $\mu_0 = 1$ GeV.

Since $a_{27}(\mu)$ is a CP-conserving parameter, Eq. (41) allows us to predict also the tiny CP-violating component of g_{27} . Taking the experimental value of $\text{Re}[g_{27}]$ in Eq. (52), one gets

$$\text{Im}[g_{27}] = \frac{\text{Im}\left(C_1 + C_2 + \frac{3}{2}C_9 + \frac{3}{2}C_{10}\right)}{\text{Re}\left(C_1 + C_2 + \frac{3}{2}C_9 + \frac{3}{2}C_{10}\right)} \text{Re}[g_{27}] = -(0.0037 \pm 0.0002) \text{Im}(\tau), \quad (60)$$

where $\text{Im}(\tau) \approx -\eta\lambda^4 A^2 / \sqrt{1 - \lambda^2}$ in the Wolfenstein parametrization of the CKM matrix.

⁷ $B_K(\mu)$ receives large chiral corrections of $\mathcal{O}[M_K^2 \log(M_K^2/\nu_\chi^2)/\Lambda_\chi^2]$ [14].

4 Vacuum condensates

The two-point correlation functions of the colour-singlet vector $V_{ij}^\mu = \bar{q}^j \gamma^\mu q_i$ and axial-vector $A_{ij}^\mu = \bar{q}^j \gamma^\mu \gamma_5 q_i$ quark currents,

$$\Pi_{ij,\mathcal{J}}^{\mu\nu}(q) \equiv i \int d^4x e^{iqx} \langle 0 | T(\mathcal{J}_{ij}^\mu(x) \mathcal{J}_{ij}^\nu(0)^\dagger) | 0 \rangle = (-g^{\mu\nu} q^2 + q^\mu q^\nu) \Pi_{ij,\mathcal{J}}^{L+T}(q^2) + g^{\mu\nu} q^2 \Pi_{ij,\mathcal{J}}^L(q^2), \quad (61)$$

play a central role in the study of hadronic production through electroweak currents [8]. Here, $\mathcal{J} = V, A$ and the superscripts denote the transverse (T) and longitudinal (L) components. We are mainly interested in the correlators associated with \mathcal{J}_{ud}^μ , $(V + A)_{us}^\mu$ and $\bar{J}_{\text{em}}^\mu \equiv \sqrt{3/2} \sum_i e_i V_{ii}^\mu$, which can be related to precise experimental data. From now on, we focus on their corresponding $L + T$ parts (omitting the $L + T$ label), which we will denote $\Pi_{\mathcal{J}}^d$, Π_{V+A}^s and $\bar{\Pi}_{EM}$.

At large Euclidean momenta $Q^2 = -q^2 \gg \Lambda_{\text{QCD}}^2$, their asymptotic behaviour is well described by the OPE [12]:

$$\Pi(q^2) = \sum_{i,D} \frac{C_{i,D}(q^2, \mu) \langle \mathcal{O}_{i,D}(\mu) \rangle}{(-q^2)^{D/2}} \equiv \sum_D \frac{\langle \mathcal{O}_D \rangle}{(-q^2)^{D/2}}. \quad (62)$$

The leading $D = 0$ perturbative contribution, which is currently known to order α_s^4 [58–61], is corrected by inverse-power contributions from gauge- and Lorentz-invariant operators of increasing dimension D . These dimensional corrections, obtained by dressing and renormalizing contributions where not all quark and gluon fields are contracted, are characterized by Wilson coefficients that only depend logarithmically on the energy scale,

$$C_{i,D}(q^2, \mu) = C_{i,D}^0 \left\{ 1 + \alpha_s(\mu) [c_{i,D} + c_{i,D}^L \log(-q^2/\mu^2)] + \mathcal{O}(\alpha_s^2) \right\}, \quad (63)$$

where the coefficients $c_{i,D}^L$ are related to the leading anomalous-dimension matrix of the associated operators.

We are going to analyze the four-quark operators that appear at $D = 6$. Following a notation close to Eqs. (4) and (25), their contributions to the relevant current correlators [11] can be written in the form⁸

$$\begin{aligned} \mathcal{O}_6 = & [\tilde{t}_L]_{ik}^{jl} (\bar{q}_L^i \gamma^\mu T^a q_{Lj}) (\bar{q}_L^k \gamma_\mu T^a q_{Ll}) + [\tilde{t}_R]_{ik}^{jl} (\bar{q}_R^i \gamma^\mu T^a q_{Rj}) (\bar{q}_R^k \gamma_\mu T^a q_{Rl}) \\ & + [t_{LR}^{\delta\delta}]_{ik}^{jl} (\bar{q}_L^i \gamma^\mu q_{Lj}) (\bar{q}_R^k \gamma_\mu q_{Rl}) + [t_{LR}^{\lambda\lambda}]_{ik}^{jl} (\bar{q}_L^i \gamma^\mu T^a q_{Lj}) (\bar{q}_R^k \gamma_\mu T^a q_{Rl}). \end{aligned} \quad (64)$$

⁸For the left-left and right-right operators, the notation of Eq. (4) without colour matrices corresponds to $[t_{L(R)}]_{ik}^{jl} = \frac{1}{2} \left([\tilde{t}_{L(R)}]_{ik}^{lj} - \frac{1}{N_C} [\tilde{t}_{L(R)}]_{ik}^{jl} \right)$.

At LO in α_s , $[t_{LR}^{\delta\delta}]_{ik}^{jl} = 0$. For $\Pi_{\mathcal{J}}^d$ the non-zero tensor coefficients are

$$[\tilde{t}_{L,\mathcal{J}}^d]_{ik}^{jl} = [\tilde{t}_{R,\mathcal{J}}^d]_{ik}^{jl} = -8\pi\alpha_s \left\{ \frac{1}{4} (\lambda_i^{1,j} \lambda_k^{1,l} + \lambda_i^{2,j} \lambda_k^{2,l}) + \frac{1}{18\sqrt{3}} (\lambda_i^{8,j} \delta_k^l + \lambda_k^{8,l} \delta_i^j) + \frac{2}{27} \delta_i^j \delta_k^l \right\}, \quad (65)$$

$$[t_{LR,\mathcal{J}}^{d,\lambda\lambda}]_{ik}^{jl} = -8\pi\alpha_s \left\{ \mp \frac{1}{2} (\lambda_i^{1,j} \lambda_k^{1,l} + \lambda_i^{2,j} \lambda_k^{2,l}) + \frac{1}{9\sqrt{3}} (\lambda_i^{8,j} \delta_k^l + \lambda_k^{8,l} \delta_i^j) + \frac{4}{27} \delta_i^j \delta_k^l \right\}, \quad (66)$$

where the upper (lower) signs correspond to the vector (axial-vector) currents. To obtain the corresponding results for the $\Pi_{\mathcal{J}}^s$ correlators, one just needs to exchange the down and strange quarks, which amounts to the changes

$$[t_{\mathcal{J}}^s]_{ik}^{jl} = [t_{\mathcal{J}}^d]_{ik}^{jl} \left(\lambda_1 \rightarrow \lambda_4, \lambda_2 \rightarrow \lambda_5, \lambda_8 \rightarrow \frac{\sqrt{3}}{2} (\lambda_3 - \frac{1}{\sqrt{3}} \lambda_8) \right). \quad (67)$$

Finally, the tensor coefficients of the electromagnetic correlator $\bar{\Pi}_{EM}$ are

$$[\tilde{t}_{L,EM}]_{ik}^{jl} = [\tilde{t}_{R,EM}]_{ik}^{jl} = -8\pi\alpha_s \left\{ \frac{3}{2} Q_i^j Q_k^l + \frac{1}{18} (Q_i^j \delta_k^l + \delta_i^j Q_k^l) + \frac{2}{27} \delta_i^j \delta_k^l \right\}, \quad (68)$$

$$[t_{LR,EM}^{\lambda\lambda}]_{ik}^{jl} = -8\pi\alpha_s \left\{ -3 Q_i^j Q_k^l + \frac{1}{9} (Q_i^j \delta_k^l + \delta_i^j Q_k^l) + \frac{4}{27} \delta_i^j \delta_k^l \right\}. \quad (69)$$

In addition to the octet and 27-plet structures, all these correlators contain also flavour-singlet components. However, the singlet terms cancel in the flavour-breaking differences Π_{V-A}^d , Π_{V+A}^{d-s} and $\bar{\Pi}_{EM} - \Pi_V^d$, together with the purely perturbative contributions.⁹ These correlation functions are then governed by long-distance matrix elements that can be related to the ones discussed in the previous section.

4.1 $\mathcal{O}_{6,V-A}^d$

The cleanest flavour-breaking difference is $\mathcal{O}_{6,V-A}^d$, which only receives an $(8_L, 8_R)$ contribution from $[t_{LR,V-A}^{d,\lambda\lambda}]_{ik}^{jl} = 8\pi\alpha_s (\lambda_{L,i}^{1,j} \lambda_{R,k}^{1,l} + \lambda_{L,i}^{2,j} \lambda_{R,k}^{2,l})$. From Eqs. (25) and (29), the realization of this local operator in terms of the long-distance degrees of freedom is found to be:

$$\mathcal{O}_{6,V-A}^d(\mu) = 8\pi\alpha_s(\mu) F^6 a_{88}^{\lambda\lambda}(\mu) \text{Tr}(\lambda_L^1 U^\dagger \lambda_R^1 U + \lambda_L^2 U^\dagger \lambda_R^2 U) + \mathcal{O}(p^2, \alpha_s^2). \quad (70)$$

Taking now the vacuum expectation value, one finds

$$\langle \mathcal{O}_{6,V-A}^d(\mu) \rangle = 32\pi\alpha_s(\mu) F^6 a_{88}^{\lambda\lambda}(\mu) + \mathcal{O}(p^2, \alpha_s^2), \quad (71)$$

which provides a direct link between this condensate and $g_8 g_{\text{ewk}}$ in Eq. (43).

⁹The so-called singlet topologies that only contribute to the neutral correlators are absent in the three-flavour theory because $\sum_q e_q = 0$ [8].

Expanding the flavour trace in Eq. (70) to second order in the Goldstone fields and computing the resulting tadpole contributions, we can easily obtain the $\mathcal{O}(p^2)$ χ PT corrections to the vacuum condensate:

$$\begin{aligned} \langle \mathcal{O}_{6,V-A}^d(\mu) \rangle &= 32\pi\alpha_s(\mu) F^6 a_{88}^{\lambda\lambda}(\mu) \left\{ 1 - \frac{2M_K^2}{(4\pi F)^2} \log\left(\frac{M_K^2}{\nu_\chi^2}\right) - \frac{4M_\pi^2}{(4\pi F)^2} \log\left(\frac{M_\pi^2}{\nu_\chi^2}\right) \right. \\ &\quad \left. + \frac{4}{F^2} M_\pi^2 c_4^{\lambda\lambda}(\nu_\chi, \mu) + \frac{2}{F^2} (2M_K^2 + M_\pi^2) c_6^{\lambda\lambda}(\nu_\chi, \mu) \right\} + \mathcal{O}(p^4, \alpha_s^2). \end{aligned} \quad (72)$$

The chiral logarithmic corrections are unambiguously predicted in terms of the LO coupling $a_{88}^{\lambda\lambda}(\mu)$, but there are in addition local contributions from the $\mathcal{O}(p^2)$ χ PT operators [62]

$$\begin{aligned} \mathcal{L}_{8L,8R}^{\mathcal{O}(p^4)} &= \frac{F^4}{4} c_4^{\lambda\lambda} [t_{LR}^{\lambda\lambda}]^{jl} \lambda_{L,j}^{a,i} \lambda_{R,l}^{b,k} \text{Tr}(\lambda_L^a S_+ U^\dagger \lambda_R^b U + \lambda_L^a U^\dagger \lambda_R^b U S_+) \\ &\quad + \frac{F^4}{4} c_6^{\lambda\lambda} [t_{LR}^{\lambda\lambda}]^{jl} \lambda_{L,j}^{a,i} \lambda_{R,l}^{b,k} \text{Tr}(\lambda_L^a U^\dagger \lambda_R^b U) \text{Tr}(S_+), \end{aligned} \quad (73)$$

with $S_+ = U^\dagger \chi + \chi^\dagger U$. The renormalized couplings $c_{4,6}^{\lambda\lambda}(\nu_\chi, \mu)$ reabsorb the loop divergences and, therefore, depend on both the short-distance (μ) and χ PT (ν_χ) renormalization scales:

$$c_i^{\lambda\lambda,(0)}(\mu) = a_{88}^{\lambda\lambda}(\mu) \left\{ c_i^{\lambda\lambda,r}(\nu_\chi, \mu) + \frac{\zeta_i}{(4\pi F)^2} \left[\frac{2\nu_\chi^{D-4}}{D-4} + \gamma_E - \log(4\pi) - 1 \right] \right\}, \quad (74)$$

where $\zeta_4 = \frac{3}{4}$ and $\zeta_6 = \frac{1}{2}$. These couplings can be easily estimated in the large- N_C limit, using Eq. (34):

$$c_4^{\lambda\lambda,\infty}(\nu_\chi, \mu) = 2(2L_8 + H_2) = \frac{32}{3} L_8, \quad c_6^{\lambda\lambda,\infty}(\nu_\chi, \mu) = 0. \quad (75)$$

The dependence of the product $a_{88}^{\lambda\lambda,\infty}(\mu) c_4^{\lambda\lambda,\infty}(\nu_\chi, \mu)$ on the short-distance renormalization scale μ is fully carried by $a_{88}^{\lambda\lambda,\infty}(\mu)$, through the factor $B(\mu)$ in Eq. (36), while the dependence on the scale ν_χ is of higher order in $1/N_C$ because it is a χ PT loop effect.

The NLO corrections in α_s are also known [63, 64]. For $\mathcal{O}_{6,V-A}^d$ they have the structure:

$$[t_{LR}^{\delta\delta}]^{jl} = \alpha_s^2 \left[A_1 + B_1 \log\left(\frac{-q^2}{\mu^2}\right) \right] (\lambda_{L,i}^{1,j} \lambda_{R,k}^{1,l} + \lambda_{L,i}^{2,j} \lambda_{R,k}^{2,l}), \quad (76)$$

$$[t_{LR}^{\lambda\lambda}]^{jl} = 8\pi\alpha_s \left[1 + \frac{\alpha_s}{2\pi} A_8 + \frac{\alpha_s}{2\pi} B_8 \log\left(\frac{-q^2}{\mu^2}\right) \right] (\lambda_{L,i}^{1,j} \lambda_{R,k}^{1,l} + \lambda_{L,i}^{2,j} \lambda_{R,k}^{2,l}), \quad (77)$$

where [63–65]

$$B_1 = 3 \left(1 - \frac{1}{N_C^2} \right), \quad B_8 = \frac{n_f - N_C}{3} - \frac{3}{N_C}, \quad (78)$$

are related to the anomalous dimensions of the four-quark operators, with $n_f = 3$ quark flavours. The values of the non-logarithmic coefficients A_1 and A_8 depend on the adopted

regularization prescription for γ_5 . The most recent calculation gives, in the naive dimensional regularization (NDR) and 't Hooft-Veltman (HV) schemes [28]:

$$A_1 = \begin{cases} 2 & \text{(NDR)} \\ -10/3 & \text{(HV)} \end{cases}, \quad A_8 = \begin{cases} 25/4 & \text{(NDR)} \\ 21/4 & \text{(HV)} \end{cases}, \quad (79)$$

for $n_f = N_C = 3$. These NLO QCD corrections introduce the colour-singlet four-quark left-right operator and, therefore, additional non-perturbative parameters. The final expression for the vacuum condensate at NLO in χ PT and α_s is then given by

$$\begin{aligned} \langle \mathcal{O}_{6,V-A}^d(\mu) \rangle &= 32\pi\alpha_s(\mu) F^6 a_{88}^{\lambda\lambda}(\mu) \left[1 + \frac{\alpha_s(\mu)}{2\pi} A_8 + \frac{\alpha_s(\mu)}{2\pi} B_8 \log\left(\frac{-q^2}{\mu^2}\right) \right] \\ &\cdot \left\{ 1 - \frac{2M_K^2}{(4\pi F)^2} \log\left(\frac{M_K^2}{\nu_\chi^2}\right) - \frac{4M_\pi^2}{(4\pi F)^2} \log\left(\frac{M_\pi^2}{\nu_\chi^2}\right) \right. \\ &\quad \left. + \frac{4}{F^2} M_\pi^2 c_4^{\lambda\lambda}(\nu_\chi, \mu) + \frac{2}{F^2} (2M_K^2 + M_\pi^2) c_6^{\lambda\lambda}(\nu_\chi, \mu) \right\} \\ &+ 4\alpha_s^2(\mu) F^6 a_{88}^{\delta\delta}(\mu) \left[A_1 + B_1 \log\left(\frac{-q^2}{\mu^2}\right) \right] \\ &\cdot \left\{ 1 - \frac{2M_K^2}{(4\pi F)^2} \log\left(\frac{M_K^2}{\nu_\chi^2}\right) - \frac{4M_\pi^2}{(4\pi F)^2} \log\left(\frac{M_\pi^2}{\nu_\chi^2}\right) \right. \\ &\quad \left. + \frac{4}{F^2} M_\pi^2 c_4^{\delta\delta}(\nu_\chi, \mu) + \frac{2}{F^2} (2M_K^2 + M_\pi^2) c_6^{\delta\delta}(\nu_\chi, \mu) \right\}. \quad (80) \end{aligned}$$

The contribution from the colour-singlet four-quark operator is nevertheless very small. In addition to be a higher-order correction in the strong coupling, it is colour suppressed. In the large- N_C limit,

$$a_{88}^{\delta\delta,\infty}(\mu) = c_4^{\delta\delta,\infty}(\nu_\chi, \mu) = c_6^{\delta\delta,\infty}(\nu_\chi, \mu) = 0. \quad (81)$$

In order to keep track of the total size of the chiral logarithmic corrections, which will be useful to estimate uncertainties in the comparison with the kaon sector in Section 6, it is convenient to rewrite Eq. (80) reabsorbing the chiral logarithms into powers of F/F_π . Doing that and approximating the NLO counterterms, which play a very minor numerical role, by their large- N_c values, one finds:

$$\begin{aligned} \langle \mathcal{O}_{6,V-A}^d(\mu) \rangle &= 32\pi\alpha_s(\mu) F_\pi^4 \left\{ F^2 a_{88}^{\lambda\lambda}(\mu) \left[1 + \frac{\alpha_s(\mu)}{2\pi} A_8 + \frac{\alpha_s(\mu)}{2\pi} B_8 \log\left(\frac{-q^2}{\mu^2}\right) \right] \right. \\ &\quad \left. + F^2 a_{88}^{\delta\delta}(\mu) \frac{\alpha_s(\mu)}{8\pi} \left[A_1 + B_1 \log\left(\frac{-q^2}{\mu^2}\right) \right] \right\} \left\{ 1 - \frac{16M_\pi^2}{F_\pi^2} \left(L_5 - \frac{8}{3} L_8 \right) \right\}. \quad (82) \end{aligned}$$

4.2 Other flavour-breaking structures

The bosonization of $\mathcal{O}_{6,V+A}^{d-s}$ can be obtained with the same method. However, the $(8_L, 8_R)$ structures disappear when summing the vector and axial-vector contributions, as can be

seen in Eq. (66). This implies that the corresponding effective operator contains two derivatives and, therefore, cannot acquire a vacuum expectation value at tree-level. The associated $\mathcal{O}_{6,V+A}^{d-s}$ condensate can be only generated through χ PT loops and is then heavily suppressed with respect to $\mathcal{O}_{6,V-A}^d$ by a factor of $\mathcal{O}(M_K^4/\Lambda_\chi^4)$.

The bosonization of $\mathcal{O}_{6,EM} - \mathcal{O}_{6,V}^d$ contains an $\mathcal{O}(p^0)$ term proportional to $a_{88}^{\lambda\lambda}$, generated by the $[t_{LR}^{\lambda\lambda}]$ contribution. However, the vacuum expectation value of this term also vanishes at tree-level and, as a consequence, it has a chiral suppression of $\mathcal{O}(M_K^2/\Lambda_\chi^2)$. This suppression is not accidental. The currents \bar{J}_{EM}^μ and $J_{ud,V}^\mu$ are trivially related by an $SU(3)_V$ rotation. Their two-point correlation functions $\bar{\Pi}_{EM}^d$ and Π_V^d must then be identical, as far as the $SU(3)_V$ symmetry is preserved. But $SU(3)_V$ cannot be spontaneously broken in QCD [66]. Any nonzero condensate in the difference must then emerge as a consequence of an explicit symmetry breaking of $SU(3)_V$, which is fully dominated by the nonzero strange quark mass, leading to an $\mathcal{O}(M_K^2/\Lambda_\chi^2)$ suppression.

5 Determination of $\text{Im}(g_8 g_{\text{ewk}})$ from τ -decay data

The inclusive invariant-mass distributions of the final hadrons in τ decay directly measure the hadronic spectral functions associated with the ud and us two-point current correlators in Eq. (61), up to the τ mass scale [8, 11]:

$$\frac{d\Gamma}{ds} = \frac{G_F^2}{16\pi^2} m_\tau^3 S_{\text{EW}} \left(1 - \frac{s}{m_\tau^2}\right)^2 \left\{ \left(1 + 2 \frac{s}{m_\tau^2}\right) \text{Im} \Pi_\tau^{L+T}(s) - 2 \frac{s}{m_\tau^2} \text{Im} \Pi_\tau^L(s) \right\}, \quad (83)$$

where

$$\Pi_\tau(s) \equiv \sum_{i=d,s} |V_{ui}|^2 [\Pi_{ui,V}(s) + \Pi_{ui,A}(s)] \quad (84)$$

and $S_{\text{EW}} = 1.0201 \pm 0.003$ incorporates the (renormalization-group improved) electroweak corrections [67–69]. Identifying an even or odd number of pions and kaons in the final state, one can further separate the spectral distributions corresponding to V_{ud} , A_{ud} and $V_{us} + A_{us}$.

We are going to focus in the Cabibbo-allowed ud spectral functions, making use of the most precise measurements of the corresponding vector and axial-vector distributions, extracted from ALEPH data [70], which are displayed in Fig. 1. Given the current experimental uncertainties, the longitudinal axial spectral function is well approximated by the pion pole contribution, $\text{Im}\Pi_A^L(s) = 2\pi F_\pi^2 \delta(s - m_\pi^2)$, while the tiny contribution from $\text{Im}\Pi_V^L(s)$ can be safely neglected.

The current correlators are analytic functions in all the complex $s \equiv q^2$ plane, except for the physical cut in the positive real axis where they acquire their absorptive components. Apart from the pion pole, this cut starts at $s_{\text{th}} = 4M_\pi^2$. Integrating along the circuit of Fig. 2 a given correlator times any arbitrary weight function $\omega(s)$, analytic at least in the

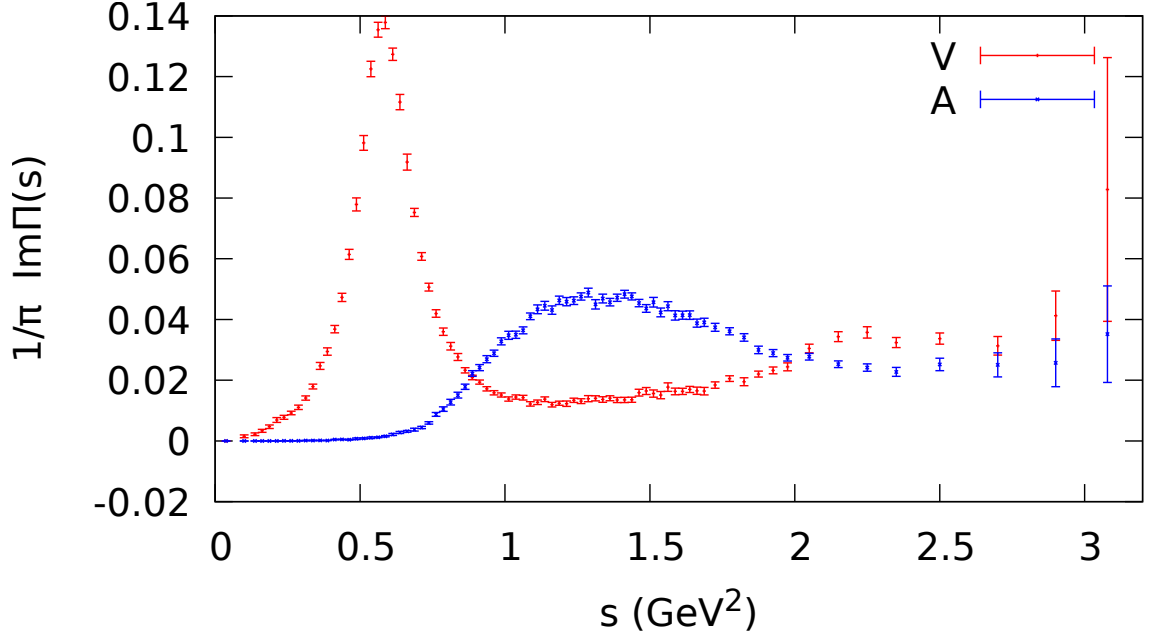


Figure 1: ALEPH non-strange spectral functions $\frac{1}{\pi} \text{Im} \Pi_{ud,V/A}^{L+T}(s)$.

same complex region as the correlator, one finds

$$\int_{s_{\text{th}}}^{s_0} \frac{ds}{s_0} \omega(s) \frac{1}{\pi} \text{Im} \Pi^{L+T}(s) + \frac{1}{2\pi i} \oint_{|s|=s_0} \frac{ds}{s_0} \omega(s) \Pi^{L+T}(s) = 2 \frac{F_\pi^2}{s_0} \omega(M_\pi^2). \quad (85)$$

In the first term one can introduce the experimental spectral function, while for large enough values of s_0 , the OPE of $\Pi^{L+T}(s)$ becomes an excellent approximation for the integral along the complex circle $|s| = s_0$, except maybe for the region near the positive real axis [11, 71].

The small differences between using the physical correlators or their OPE approximations are known as quark-hadron duality violations [29, 72–78]:

$$\begin{aligned} \delta_{\text{DV}}[\omega(s), s_0] &\equiv \frac{1}{2\pi i} \oint_{|s|=s_0} \frac{ds}{s_0} \omega(s) [\Pi^{L+T}(s) - \Pi_{\text{OPE}}^{L+T}(s)] \\ &= \frac{1}{\pi} \int_{s_0}^{\infty} \frac{ds}{s_0} \omega(s) [\text{Im} \Pi^{L+T}(s) - \text{Im} \Pi_{\text{OPE}}^{L+T}(s)]. \end{aligned} \quad (86)$$

These effects get strongly suppressed when using (pinched) weight functions $\omega(s)$ with zeros at $s = s_0$. This can be seen in two different ways. First, the zeros at $s = s_0$ kill the contributions to the contour integral from the region near the physical axis, where the OPE is less justified. Second, since $\text{Im} \Pi_{\text{OPE}}^{L+T}(s)$ approaches $\text{Im} \Pi^{L+T}(s)$ very fast, typically

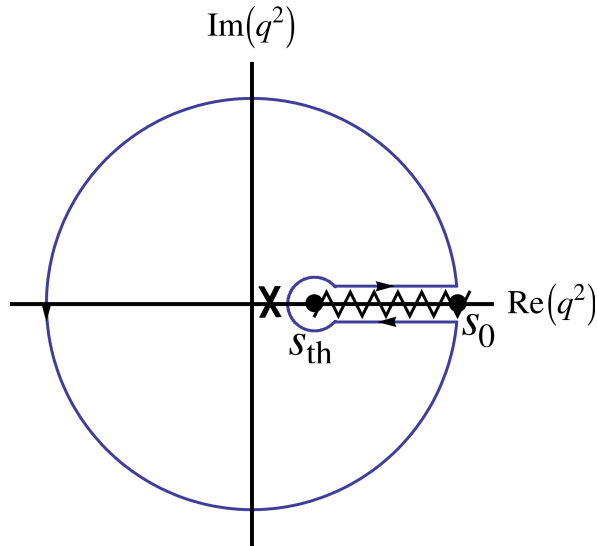


Figure 2: Analytic structure of $\Pi^{L+T}(s)$ and complex contour used to derive Eq. (85).

exponentially, the spectral differences are dominated by the region near s_0 that pinched weight functions remove.

In this work, we are interested in the correlation function $\Pi_{V-A}(s) \equiv \Pi_{ud,V}^{L+T} - \Pi_{ud,A}^{L+T}$, which vanishes to all orders in perturbation theory when quark masses are neglected. Since $m_{u,d}$ are tiny, this is an excellent approximation in the up-down sector. The non-zero value of $\Pi(s)$ originates in the spontaneous breaking of chiral symmetry by the QCD vacuum, which results in different vector and axial-vector correlators. The leading OPE contribution comes from four-quark operators with $D = 6$ (the lowest dimension where a chiral-symmetry breaking can be induced with massless quark and gluon fields) and is suppressed by six powers of the τ mass. Although the vector and axial-vector spectra in Fig. 1 have very different shapes in the low-energy resonance regime, chiral symmetry implies a very strong suppression of their integrated difference in Eq. (85) when duality violations are suppressed, *i.e.*, taking s_0 near m_τ^2 and pinched weight functions.

In order to illustrate this, let us focus on the pinched integrals

$$F_{V\pm A}(s_0) \equiv \int_{s_{\text{th}}}^{s_0} \frac{ds}{s_0} \left(1 - \frac{s}{s_0}\right) \frac{1}{\pi} \text{Im} \Pi_{V\pm A}(s) \pm 2 \frac{F_\pi^2}{s_0} \left(1 - \frac{m_\pi^2}{s_0}\right), \quad (87)$$

which are plotted in Fig. 3, as a function of the upper integration limit s_0 . In spite of the very small experimental uncertainties, which are below the percent level, no signatures of non-perturbative effects can be observed near the τ mass. $F_{V-A} \approx 0$, as expected, exhibiting the negligible role of duality violations in this pinched observable, at large s_0 . While for the $V+A$ channel this fact leads to a precise determination of the strong coupling [11, 70, 79, 80], it also translates into a very limited sensitivity to the gluon and four-quark condensates. Since four-quark operators only enter into the integral (87) through the α_s -suppressed logarithmic term in Eq. (62), they could only leave a sizeable imprint at very

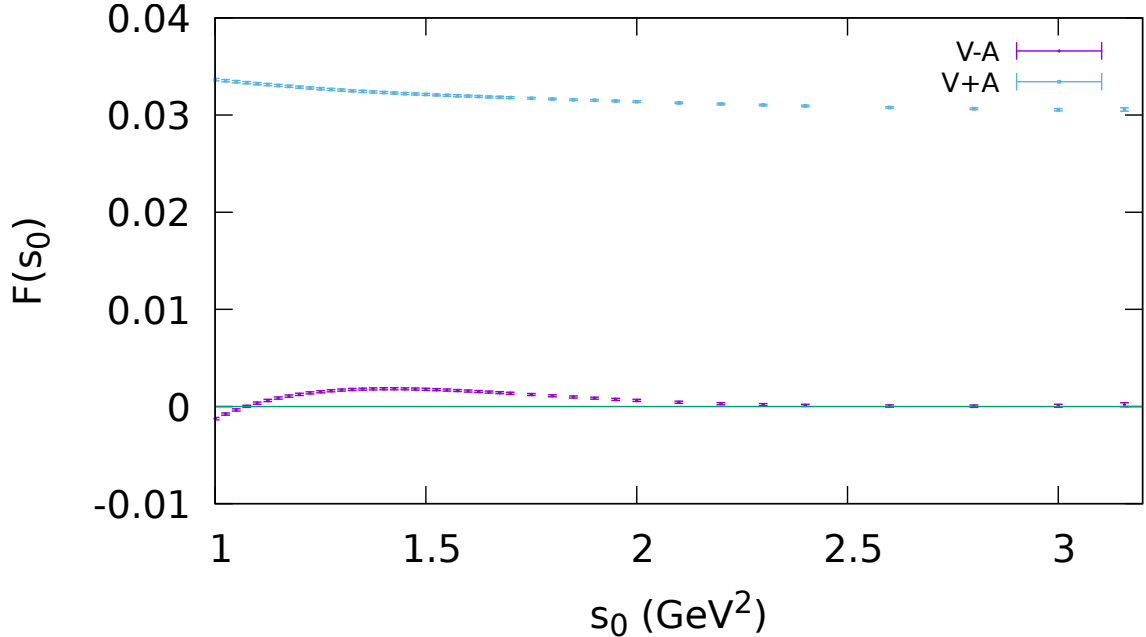


Figure 3: $F_{V\pm A}(s_0)$ as defined in Eq. (87). The upper and lower curves correspond to $V + A$ and $V - A$, respectively.

small values of s_0 , where duality violations are beyond theoretical control, as becomes manifest looking at the large splitting of the spectra in Fig. 1.

Taking into account the current experimental uncertainties and provided the renormalization scale μ is set close to the tau mass, one can neglect the running of the QCD corrections and work with effective condensates $\langle \mathcal{O}_D \rangle$ in Eq. (62), independent of the energy scale.¹⁰ Inserting the OPE into the second term of Eq. (85) and invoking the Cauchy formula, every monomial weight function $\omega(s) = (s/s_0)^n$ becomes connected to a different effective condensate $\langle \mathcal{O}_{2(n+1)} \rangle$. For the $V - A$ correlation function, one finds

$$\int_{s_{\text{th}}}^{s_0} \frac{ds}{s_0} \left(\frac{s}{s_0} \right)^n \frac{1}{\pi} \text{Im} \Pi_{V-A}(s) + (-1)^{n+1} \frac{\langle \mathcal{O}_{2(n+1)} \rangle}{s_0^{n+1}} + \delta_{\text{DV}}[(s/s_0)^n, s_0] = 2 \frac{F_\pi^2}{s_0} \left(\frac{M_\pi^2}{s_0} \right)^n. \quad (88)$$

Determining $\langle \mathcal{O}_6 \rangle$, which is nothing else but $\langle \mathcal{O}_{6,V-A}^d(s_0) \rangle$ in Eq. (82),¹¹ is going to give us $a_{88}^{\lambda\lambda}(s_0)$, which is linked to $e^2 g_8 g_{\text{ewk}}(s_0)$ through Eq. (43).

¹⁰The only large NLO correction in α_s , arising from the large value of A_8 in eq. (82), does not change this approximation and will be taken into account.

¹¹The scale is set to s_0 in order to avoid large logarithms in the α_s corrections.

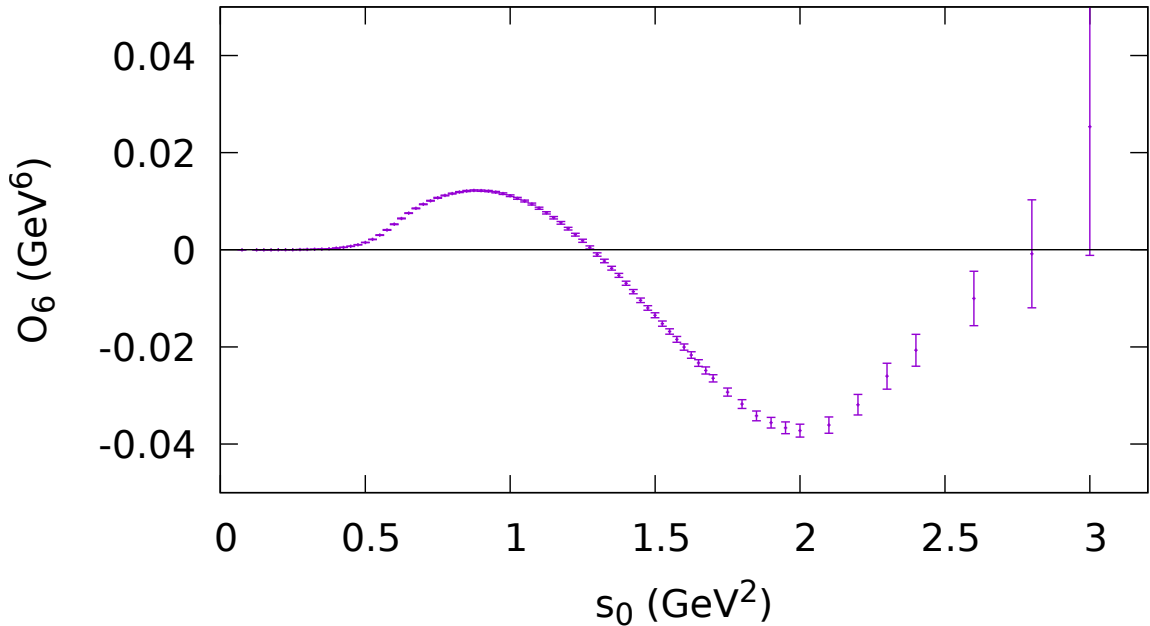


Figure 4: Rescaled version of the moment associated to $\omega(s) = (s/s_0)^2$ so that, at large-enough s_0 , it converges to $\langle \mathcal{O}_6 \rangle$.

5.1 Determination of $\langle \mathcal{O}_6 \rangle$

We already determined $\langle \mathcal{O}_6 \rangle$ in Ref. [81], which updated Refs. [76, 77]. In this subsection we revisit it, introducing some minor modifications and extra tests.

5.1.1 Determination of $\langle \mathcal{O}_6 \rangle$ based on energy stability

Naively, one could try to estimate $\langle \mathcal{O}_6 \rangle$ by using Eq. (88) with the corresponding monomial function $\omega(s) = (s/s_0)^2$, hoping that at large-enough energies duality violations are negligible. This should be reflected in the appearance of a plateau at high energies, when making the trivial rescaling of that equation, so that it converges to $\langle \mathcal{O}_6 \rangle$ for large-enough values of s_0 . However, as can be seen in Fig. 4, there are large violations of quark–hadron duality and the experimental uncertainties grow when increasing s_0 . The weight function is enhancing both the contribution of the high-energy part of the spectral function, where data are less precise, and the high-energy duality-violation tail associated to Eq. (86).

As already mentioned before, duality violations can be suppressed introducing pinched weight functions, containing the desired monomia. Taking the (once-pinched) $\omega(s) = x(1-x)$ and (double-pinched) $\omega(s) = (1-x)^2$ weight functions, with $x = s/s_0$, we obtain the values of $\langle \mathcal{O}_6 \rangle$ shown in Fig. 5, to be compared with Fig. 4 (notice the different scales in the y axes). Experimental uncertainties are clearly reduced and a plateau has

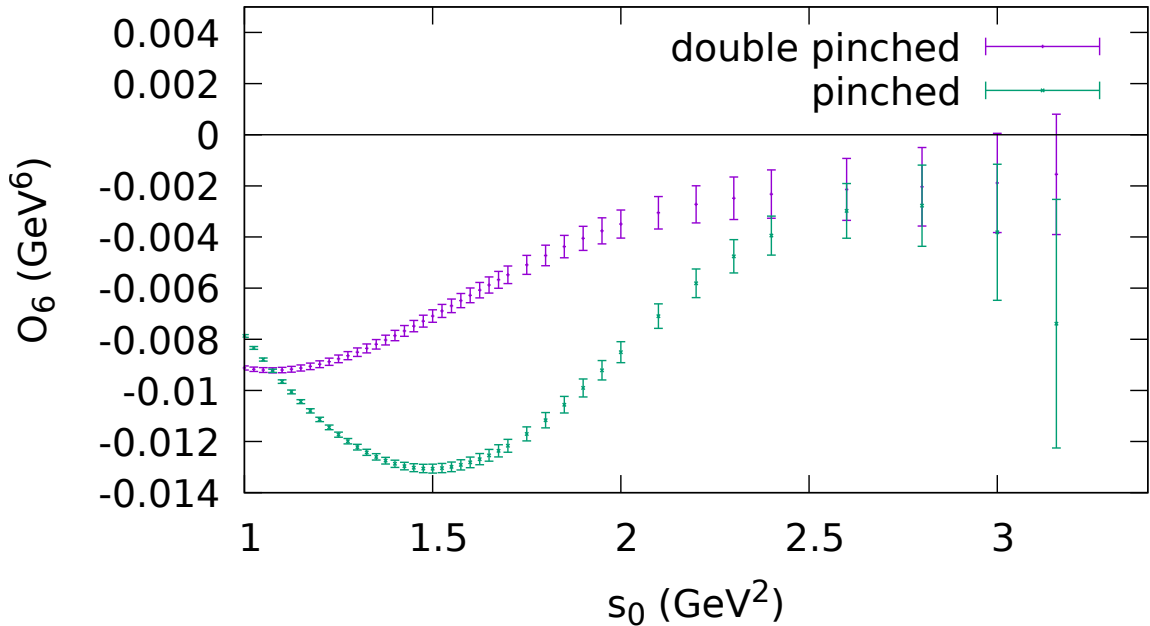


Figure 5: Results for $\langle \mathcal{O}_6 \rangle$, as a function of s_0 , obtained from (appropriately rescaled) moments with pinched weights.

arisen. One may still argue, by taking an artificial shape for the high-energy tail of the spectral function, that the plateau could be accidental and disappear at higher values of s_0 . However, since there is an increasing hadronic multiplicity at $s_0 \sim m_\tau^2$, duality violations should go to zero very fast when increasing the energy, making this contrived scenario very unlikely. Moreover, the results from the two pinched weight functions approach the same value of $\langle \mathcal{O}_6 \rangle$ at large s_0 . Thus, duality violations become indeed relatively small at large s_0 , specially for the doubly-pinched weight that leads to smaller uncertainties. Taking that into account, we take as central value the lowest energy point within the plateau, *i.e.*, the lowest one which lies within the experimental error bars of the following ones ($s_0 = 2.1 \text{ GeV}^2$), and as an estimate of duality-violation uncertainties its difference with the last energy point with an acceptable experimental resolution, *i.e.*, $s_0 = 2.8 \text{ GeV}^2$. We obtain in this way

$$\langle \mathcal{O}_6 \rangle^{\text{stab}} = (-3.1 \pm 0.6_{\text{exp}} \pm 1.0_{\text{DV}}) \cdot 10^{-3} \text{ GeV}^6 = (-3.1 \pm 1.2) \cdot 10^{-3} \text{ GeV}^6. \quad (89)$$

5.1.2 Determination of $\langle \mathcal{O}_6 \rangle$ modeling duality violations

An alternative approach to estimate duality-violation effects consists in trying to guess the spectral function $\rho(s) = \frac{1}{\pi} \text{Im} \Pi_{V-A}(s)$ above the region where data are available.¹² In

¹²At LO in α_s , $\rho_{\text{DV}}(s) = \rho(s)$ because the OPE does not generate absorptive contributions.

order to do that, a parametrization is unavoidable and, therefore, some model-dependence arises. We will impose the theoretical requirement that the physical spectral function must obey the Weinberg Sum Rules (WSRs) [82], *i.e.* Eq. (88) for $n = 0$ and $n = 1$, which do not involve any condensate contribution. This condition restricts very strongly the possible choice of admissible spectral functions.

We will adopt the four-parameter ansatz [74–77, 83–85]

$$\rho(s) = \frac{1}{\pi} \kappa e^{-\gamma s} \sin[\beta(s - s_z)] \quad (s > \hat{s}_0) \quad (90)$$

that combines an oscillatory function with the expected exponential suppression at large values of s .

Following the procedure of Ref. [81], we generate 10^9 random tuples of $(\kappa, \gamma, \beta, s_z)$ parameters, so that every one of them represents a possible spectral function above a threshold \hat{s}_0 . The fit to the ALEPH data does not show significant deviations (p-value above 5%) from this specific ansatz above $\hat{s}_0 = 1.25 \text{ GeV}^2$. However, the model is only motivated as an approximation at higher energies, where the hadronic multiplicity is also higher. As in Ref [81], we only accept those tuples contained within the 90% C.L. region ($\chi^2 < \chi_{\min}^2 + 7.78$) in the fit to the experimental data. By doing that, we are relaxing somewhat the model dependence by allowing small deviations of the admissible spectral functions from the fitted data.

In Ref. [81] we imposed in this step the short-distance constraints on the tuples, *i.e.*, the WSRs. However, the experimental uncertainties on these constraints become then correlated in a non-trivial way with the experimental uncertainty of the final parameters.

In order to avoid that, for every accepted spectral function, we perform a combined fit to Eq. (88) for $n = 0, 1, 2$ to extract $\langle \mathcal{O}_6 \rangle$. Then we only accept those spectral functions that are compatible with the WSRs ($n = 0, 1$), selecting only the ones whose p-values in the combined fit are larger than 5%. Every accepted spectral function gives a value of $\langle \mathcal{O}_6 \rangle$. Fig. 6 shows the statistical distribution of $\langle \mathcal{O}_6 \rangle$ values, obtained with $\hat{s}_0 = 1.7 \text{ GeV}^2$. The width of this distribution provides a good assessment of the duality-violation uncertainty.

The choice of \hat{s}_0 , the parameter separating the use in Eq. (88) of real data or the model ansatz, is somehow arbitrary. Therefore, a smooth dependence on the chosen value of \hat{s}_0 , within a large-enough range, is a minimal requirement that we should impose.¹³ Repeating our procedure with different thresholds leads to the results displayed in Table 2. The overall agreement is acceptable. We choose $\hat{s}_0 = 1.7 \text{ GeV}^2$ as our optimal threshold, large enough to have some hadronic multiplicity and small enough to be able to constrain the space of parameters. We then obtain:

$$\langle \mathcal{O}_6 \rangle^{\text{ans}} = (-3.8_{-0.9}^{+0.8} \text{ DV} \pm 0.1_{\text{exp}}) \cdot 10^{-3} \text{ GeV}^6. \quad (91)$$

¹³This is analogous to the stability condition (plateau) imposed in the previous subsection. Using the ansatz at lower \hat{s}_0 does not improve the results if the convergence of data to the model at that energy is actually worse than the convergence of data to the QCD OPE above \hat{s}_0 [80].

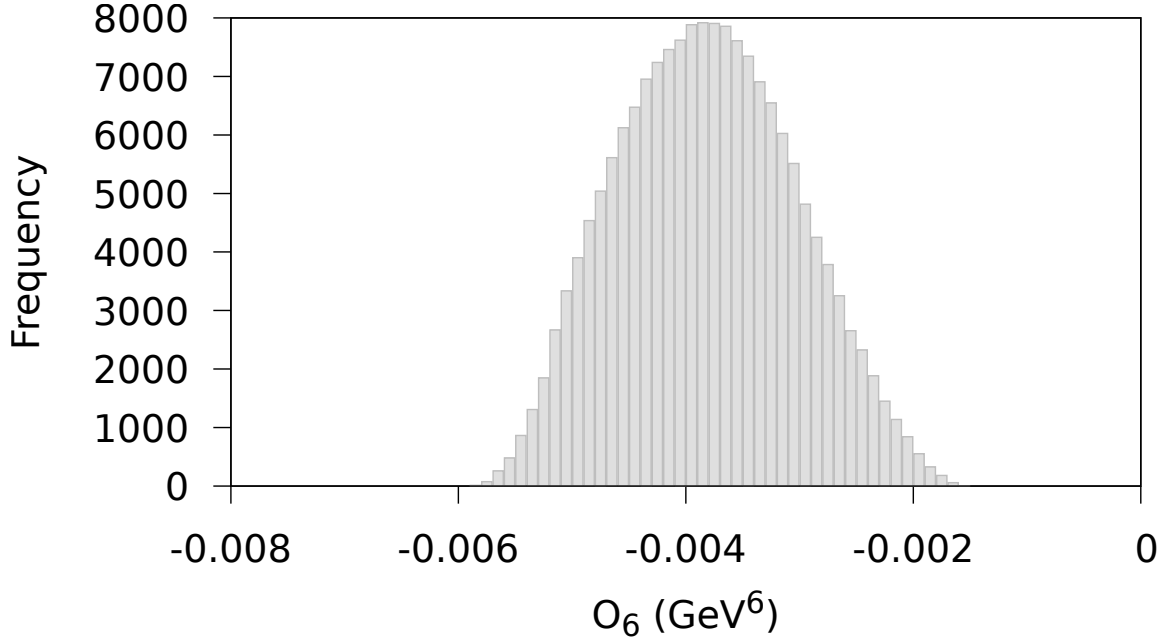


Figure 6: Distribution for $\langle \mathcal{O}_6 \rangle$ obtained with the tuples procedure at $\hat{s}_0 = 1.7 \text{ GeV}^2$.

\hat{s}_0 (GeV ²)	1.25	1.4	1.55	1.7	1.9
$\langle \mathcal{O}_6 \rangle$ (10^{-3} GeV^6)	$-5.2^{+0.5}_{-0.3}$	$-5.0^{+0.5}_{-0.5}$	$-5.3^{+0.5}_{-0.3}$	$-3.8^{+0.8}_{-0.9}$	$-3.1^{+1.0}_{-1.2}$

Table 2: Results for $\langle \mathcal{O}_6 \rangle$, obtained with our tuple procedure with different values of \hat{s}_0 .

However, even if the ansatz (90) were exactly true above some threshold \hat{s}_0 , this \hat{s}_0 could happen to be larger than the available energy range, so that the physical spectral function could not be well approximated by the fitted parameters. In that case, assuming small duality violations with double-pinch weights could be giving more accurate results than assuming the spectral function ansatz with the fitted parameters. This motivates averaging the two results. Fortunately, in this case both methods are in good agreement. Our final value, taking conservatively the quadratic sum of the lowest uncertainty plus half of the difference between central values, is:

$$\langle \mathcal{O}_{6,V-A}^d(m_\tau^2) \rangle = (-3.5 \pm 0.9) \cdot 10^{-3} \text{ GeV}^6, \quad (92)$$

in total agreement with our previous determination in Ref. [81] and the result obtained in Ref. [86] with a different procedure.

5.2 Determination of $g_8 g_{\text{ewk}}$

Inserting in Eq. (72) the obtained value for $\langle \mathcal{O}_{6,V-A}^d \rangle$, we can perform a determination of $a_{88}^{\lambda\lambda}$ at NLO in the chiral counting. We approximate the tiny counterterm piece, which has a minor numerical role, by its large- N_C estimate in Eq. (75). Incorporating also the large and dominant NLO correction in α_s coming from A_8 in Eq. (80), which does not modify the energy-independent condensate approximation used in our determination of $\langle \mathcal{O}_{6,V-A}^d \rangle$, one finds

$$F^2 a_{88}^{\lambda\lambda}(m_\tau) = (-1.15 \pm 0.30_{\langle \mathcal{O}_6 \rangle} \pm 0.11_{\text{pert}}) \text{ GeV}^2, \quad (93)$$

where we have assigned an extra 10% perturbative uncertainty based on the expected size $\sim \frac{\alpha_s(m_\tau^2)}{\pi}$ of the unaccounted NLO corrections. Notice that more precise experimental data may allow in the future for a full NLO analysis.

Taking into account that $\text{Im}(C_7)$ is smaller than $\text{Im}(C_8)$, the large N_C -suppression of $a_{88}^{\delta\delta}$ with respect to $a_{88}^{\lambda\lambda}$ and the extra $\frac{1}{N_C}$ prefactor in the contribution proportional to $C_8 a_{88}^{\delta\delta}$, we can safely neglect the $a_{88}^{\delta\delta}$ term in Eq. (43) to derive¹⁴

$$e^2 \text{Im}(g_8 g_{\text{ewk}}) \approx 12 \text{Im}[C_8(m_\tau)] a_{8L,8R}^{\lambda\lambda}(m_\tau), \quad (94)$$

from which we find

$$\frac{e^2 \text{Im}(g_8 g_{\text{ewk}})}{\text{Im}\tau} F^2 = -(1.07 \pm 0.30) \cdot 10^{-2} \text{ GeV}^2. \quad (95)$$

This phenomenological determination has a smaller central value than previous estimates, but, within the quoted uncertainties, it is in agreement with most of them [26–29, 88, 89]. As we will see in the following section, our result also agrees with the large- N_C estimate, and with the value obtained from a fit to the lattice data.

6 Interplay with $K \rightarrow \pi\pi$ transitions

As we have seen in Section 3, the $\Delta S = 1$ four-quark operators in Eq. (39) induce contributions to the corresponding LO χ Pt Lagrangian in Eq. (40), which are regulated by the couplings $a_i(\mu)$. This fully determines the $K \rightarrow \pi\pi$ matrix elements at $\mathcal{O}(p^2)$. Adopting the conventions of Ref. [87], the associated $\Delta I = \frac{1}{2}$ and $\Delta I = \frac{3}{2}$ decay amplitudes induced by the operator Q_i are easily found to be:

$$\begin{aligned} \mathcal{A}_{1/2}^{Q_i}(\mu) &\equiv \langle Q_i \rangle_{1/2} = \left(\frac{1}{9} g_{27}^{Q_i}(\mu) + g_8^{Q_i}(\mu) \right) \sqrt{2} F (M_K^2 - M_\pi^2) - \frac{2\sqrt{2}}{3} F^3 (e^2 g_8 g_{\text{ewk}})^{Q_i}(\mu), \\ \mathcal{A}_{3/2}^{Q_i}(\mu) &\equiv \langle Q_i \rangle_{3/2} = \frac{10}{9} g_{27}^{Q_i}(\mu) F (M_K^2 - M_\pi^2) - \frac{2}{3} F^3 (e^2 g_8 g_{\text{ewk}})^{Q_i}(\mu). \end{aligned} \quad (96)$$

¹⁴Since we have neglected long-distance electromagnetic contributions, no reliable estimate of the real part can be made at this point. While in general this is a good approximation due to the large enhancement of the short-distance piece with respect to the long-distance one, *i.e.*, $\alpha \log(M_W^2/\mu^2)$ vs $\alpha \log(\mu^2/M_{\rho/K}^2)$, no such logarithmic enhancement is present in $z_8(\mu)$, since the GIM mechanism sets $z_8(\mu > m_c) = 0$ [87].

The factors $g_j^{Q_i}(\mu)$, which contain the $a_i(\mu)$ couplings, can be directly obtained from Eqs. (41) (42) and (43) by simply taking $C_i(\mu) = 1$ and $C_{k \neq i}(\mu) = 0$.

At NLO in the chiral expansion one must take into account: 1) the different ways the LO realization of the operators Q_i can be combined with the rest of the χ PT building blocks to induce such a transition, and 2) new NLO building blocks with the appropriate transformation properties, which can be obtained in a similar way as it was done for the LO ones in Section 2. They generate the $\mathcal{O}(p^4)$ $\Delta S = 1$ χ PT Lagrangians of Refs. [19, 90, 91] and explicit values for their corresponding LECs N^{Q_i} , D^{Q_i} , and Z^{Q_i} can be obtained in terms of mass-independent NLO dynamical parameters. By doing that, one can keep track of both the short-distance renormalization scale μ and the chiral scale ν_χ .

In the isospin limit, the NLO $K \rightarrow \pi\pi$ amplitudes induced by the set of operators Q_i can be expressed in the form:

$$\langle Q_i \rangle_{\Delta I} = F_\pi \left\{ (M_K^2 - M_\pi^2) \left[A_{\Delta I}^{Q_i(8)} + A_{\Delta I}^{Q_i(27)} \right] - F^2 A_{\Delta I}^{Q_i(g)} \right\}, \quad (97)$$

with components ($X = 8, 27, g$)

$$A_{\Delta I}^{Q_i(X)} = \mathbf{a}_{\Delta I}^{(X)} g_X^{Q_i} \left[1 + \Delta_R^L A_{\Delta I}^{(X)} + i \Delta_I^L A_{\Delta I} + \Delta^C A_{\Delta I}^{Q_i(X)} \right] \quad (98)$$

where $\mathbf{a}_{\Delta I}^{(X)}$ are the tree-level normalizations in Eq. (96) and $g_X^{Q_i}$ the tree-level contributions induced by Q_i to the couplings $g_8^{Q_i}$, $g_{27}^{Q_i}$, and $(e^2 g_8 g_{\text{ewk}})^{Q_i}$. The dispersive and absorptive parts of the chiral loop corrections (the absorptive part fully comes from $\pi\pi$ re-scattering) are parametrized by $\Delta_R^L A_{\Delta I}^{(X)}$ and $\Delta_I^L A_{\Delta I}$, respectively, while the local counterterm contributions are included in $\Delta^C A_{\Delta I}^{Q_i(X)}$. All these NLO χ PT corrections can be taken from Ref. [87].

The re-scattering of the final pions generates large phase shifts in the $K \rightarrow (\pi\pi)_I$ decay amplitudes into the two possible final states with isospin $I = 0$ and 2:

$$\mathcal{A}_{1/2} = A_0 e^{i\chi_0}, \quad \mathcal{A}_{3/2} = A_2 e^{i\chi_2}, \quad (99)$$

where $A_{0,2}$ are real and positive if CP is conserved. In the isospin limit, the phases $\chi_{0,2}$ can be identified with the S-wave $\pi\pi$ scattering phase shifts $\delta_I^0(s)$ at $s = M_K^2$ (Watson's theorem). The absorptive contributions in Eq. (98) are given by the tree-level amplitudes times universal corrections $\Delta_I^L A_{1/2}$ and $\Delta_I^L A_{3/2}$, which only depend on the isospin quantum number and reproduce the χ PT values of the $I = 0$ and $I = 2$ $\pi\pi$ phase shifts at LO in the momentum expansion, *i.e.*, at $\mathcal{O}(p^2)$ [92]. Thus, the one-loop χ PT calculation only gives the first term in the Taylor expansion of $\sin(\delta_I^0) = \delta_I^0 + \mathcal{O}[(\delta_I^0)^3]$. This implies that $\cos(\delta_I^0) = 1$ at this χ PT order and, therefore, the NLO dispersive amplitudes and the moduli A_I are equal up to higher-order contributions: $A_I = \text{Dis}(\mathcal{A}_{\Delta I}) + \mathcal{O}(p^6)$. In the limit of isospin conservation, these quantities satisfy the relation

$$A_I = \text{Dis}(\mathcal{A}_{\Delta I}) \Theta_{\delta_I}, \quad \Theta_{\delta_I} \equiv \sqrt{1 + \tan^2(\delta_I^0)}. \quad (100)$$

Using the LO χ PT prediction for the phase shifts, this brings back the absorptive one-loop contributions that result in $\Theta_{\delta_0} = 1.10$ and $\Theta_{\delta_2} = 1.02$. Using instead the physical values of $\delta_I^0(M_K^2)$ [93], which include higher-order χ PT corrections, one gets

$$\Theta_{\delta_0} = 1.29 \pm 0.03, \quad \Theta_{\delta_2} = 1.011 \pm 0.004. \quad (101)$$

This final-state-interaction effect induces a strong 30% enhancement of the isoscalar amplitude, while the isotensor one is only modified by a mild 1% correction [92].

We can then extract the dispersive contributions $\text{Dis}(\langle Q_i \rangle_{1/2})$ and $\text{Dis}(\langle Q_i \rangle_{3/2})$ from Eq. (97) and obtain the corresponding isospin amplitudes $\langle Q_i \rangle_0 \equiv \text{Dis}(\langle Q_i \rangle_{1/2}) \Theta_{\delta_0}$ and $\langle Q_i \rangle_2 \equiv \text{Dis}(\langle Q_i \rangle_{3/2}) \Theta_{\delta_2}$ with the correction factors in Eq. (101), achieving a resummation of the large absorptive contributions. All needed ingredients can be taken from the tables of Refs. [32, 33, 87].¹⁵ At NLO in the chiral counting, the isoscalar amplitudes take the form:

$$\begin{aligned} \langle Q_1(\mu) \rangle_0 &= \sqrt{2} F_\pi (M_K^2 - M_\pi^2) \Theta_{\delta_0} \left\{ \frac{1}{10} [a_8^S(\mu) - 5 a_8^A(\mu)] \left(1 + \Delta_R^L A_{1/2}^{(8)} + \Delta_{Q_1}^C \right) \right. \\ &\quad \left. + \frac{1}{15} a_{27}(\mu) \left(1 + \Delta_R^L A_{1/2}^{(27)} + \Delta_{Q_1}^C \right) \right\}, \\ \langle Q_2(\mu) \rangle_0 &= \sqrt{2} F_\pi (M_K^2 - M_\pi^2) \Theta_{\delta_0} \left\{ \frac{1}{10} [a_8^S(\mu) + 5 a_8^A(\mu)] \left(1 + \Delta_R^L A_{1/2}^{(8)} + \Delta_{Q_1}^C \right) \right. \\ &\quad \left. + \frac{1}{15} a_{27}(\mu) \left(1 + \Delta_R^L A_{1/2}^{(27)} + \Delta_{Q_1}^C \right) \right\}, \\ \langle Q_3(\mu) \rangle_0 &= \frac{1}{\sqrt{2}} F_\pi (M_K^2 - M_\pi^2) \Theta_{\delta_0} [a_8^S(\mu) - a_8^A(\mu)] \left(1 + \Delta_R^L A_{1/2}^{(8)} \right), \\ \langle Q_5(\mu) \rangle_0 &= 4\sqrt{2} F_\pi (M_K^2 - M_\pi^2) \Theta_{\delta_0} a_{LR}^{\delta\delta}(\mu) \left(1 + \Delta_R^L A_{1/2}^{(8)} \right), \\ \langle Q_6(\mu) \rangle_0 &= 4\sqrt{2} F_\pi (M_K^2 - M_\pi^2) \Theta_{\delta_0} \left[2 a_{LR}^{\lambda\lambda}(\mu) + \frac{1}{N_c} a_{LR}^{\delta\delta}(\mu) \right] \left(1 + \Delta_R^L A_{1/2}^{(8)} + \Delta_{Q_6}^C \right), \\ \langle Q_7(\mu) \rangle_0 &= -4\sqrt{2} F_\pi \Theta_{\delta_0} F^2 a_{88}^{\delta\delta}(\mu) \left(1 + \Delta_R^L A_{1/2}^{(g)} \right), \\ \langle Q_8(\mu) \rangle_0 &= -4\sqrt{2} F_\pi \Theta_{\delta_0} \left[2 F^2 a_{88}^{\lambda\lambda}(\mu) + \frac{1}{N_c} F^2 a_{88}^{\delta\delta}(\mu) \right] \left(1 + \Delta_R^L A_{1/2}^{(g)} + \Delta_{Q_{8,0}}^C \right), \end{aligned} \quad (102)$$

while the $I = 2$ amplitudes are given by:

$$\begin{aligned} \langle Q_1(\mu) \rangle_2 &= \frac{2}{3} F_\pi (M_K^2 - M_\pi^2) \Theta_{\delta_2} a_{27}(\mu) \left(1 + \Delta_R^L A_{3/2}^{(27)} + \Delta_{Q_1}^C \right), \\ \langle Q_7(\mu) \rangle_2 &= -4 F_\pi \Theta_{\delta_2} F^2 a_{88}^{\delta\delta}(\mu) \left(1 + \Delta_R^L A_{3/2}^{(g)} \right), \\ \langle Q_8(\mu) \rangle_2 &= -4 F_\pi \Theta_{\delta_2} \left[2 F^2 a_{88}^{\lambda\lambda}(\mu) + \frac{1}{N_c} F^2 a_{88}^{\delta\delta}(\mu) \right] \left(1 + \Delta_R^L A_{3/2}^{(g)} + \Delta_{Q_{8,2}}^C \right). \end{aligned} \quad (103)$$

¹⁵Notice, however, our slightly different definition of the amplitudes $A_{\Delta I}^{Q_i(g)}$ that differs by a factor F_π^2/F^2 from the one adopted in Refs. [32, 33, 87].

The local counterterm contributions have been approximated by their large- N_C expressions [32, 33, 87]:

$$\begin{aligned}
\Delta_{Q_1}^C &= \frac{4M_\pi^2}{F_\pi^2} L_5, \\
\Delta_{Q_6}^C &= \frac{4M_K^2}{F_\pi^2} \left[2L_8 - \frac{1}{4} L_5 (1 - 16\lambda_3^{SS}) \right] + \frac{4M_\pi^2}{F_\pi^2} \left[\frac{8L_8^2}{L_5} - L_5 (3 + 4\lambda_3^{SS}) \right] + \mathcal{O}(\bar{\lambda}_i^{RR}), \\
\Delta_{Q_{8,0}}^C &= \frac{4M_K^2}{F_\pi^2} (4L_8 - L_5) + \frac{16M_\pi^2}{F_\pi^2} (2L_8 - L_5), \\
\Delta_{Q_{8,2}}^C &= \frac{8M_K^2}{F_\pi^2} (2L_8 - L_5) + \frac{4M_\pi^2}{F_\pi^2} (8L_8 - 3L_5).
\end{aligned} \tag{104}$$

The numerical values of the different loop and counterterm corrections are given in Tables 3 and 4. The uncertainties quoted for the loop contributions have been estimated by varying the chiral scale ν_χ in the interval (0.6 – 1.0) GeV. To estimate the smaller counterterm contributions, we have used the same input values for the χ PT LECs than Ref. [33]; their associated parametric uncertainties are reflected in the errors displayed in Table 4.

$\Delta_{R A_{1/2}}^L{}^{(8)}$	$\Delta_{R A_{1/2}}^L{}^{(27)}$	$\Delta_{R A_{1/2}}^L{}^{(g)}$	$\Delta_{R A_{3/2}}^L{}^{(27)}$	$\Delta_{R A_{3/2}}^L{}^{(g)}$
0.27 ± 0.05	1.02 ± 0.63	0.44 ± 0.10	0.01 ± 0.05	-0.34 ± 0.10

Table 3: Numerical values for the dispersive loop amplitudes $\Delta_{R A_{\Delta I}}^L{}^{(X)}$.

$\Delta_{Q_1}^C$	$\Delta_{Q_6}^C$	$\Delta_{Q_{8,0}}^C$	$\Delta_{Q_{8,2}}^C$
0.010 ± 0.001	0.15 ± 0.03	0.10 ± 0.06	-0.03 ± 0.06

Table 4: Numerical values for the counterterm contributions.

The matrix elements of Q_4 , Q_9 and Q_{10} are not independent because of the relations among operators given in footnote 6. Thus,

$$\begin{aligned}
\langle Q_4 \rangle_0 &= -\langle Q_1 \rangle_0 + \langle Q_2 \rangle_0 + \langle Q_3 \rangle_0, \\
\langle Q_9 \rangle_0 &= \frac{3}{2} \langle Q_1 \rangle_0 - \frac{1}{2} \langle Q_3 \rangle_0, \\
\langle Q_{10} \rangle_0 &= \frac{1}{2} \langle Q_1 \rangle_0 + \langle Q_2 \rangle_0 - \frac{1}{2} \langle Q_3 \rangle_0.
\end{aligned} \tag{105}$$

Notice that the strong penguin operators $Q_{3,4,5,6}$ cannot induce a $\Delta I = \frac{3}{2}$ transition and, therefore, their corresponding matrix elements into an $I = 2$ $\pi\pi$ final state are identically zero. Moreover, isospin symmetry implies

$$\langle Q_1 \rangle_2 = \langle Q_2 \rangle_2 = \frac{2}{3} \langle Q_9 \rangle_2 = \frac{2}{3} \langle Q_{10} \rangle_2. \tag{106}$$

Using the theoretically-estimated value of $a_{27}(\mu_0)$ in Eq. (59), one finds

$$\langle Q_1(\mu_0) \rangle_2 = 0.0058 (23)_{a_{27}}(3)_{\Delta_L}, \quad (107)$$

in the $\overline{\text{MS}}$ -NDR scheme at $\mu_0 = 1 \text{ GeV}$, where the first uncertainty is the parametric error from $a_{27}(\mu_0)$ and the second one accounts for missed subleading chiral corrections. The CP-conserving part of the amplitude A_2 is totally dominated by the contributions from the operators Q_1 and Q_2 . Taking the corresponding Wilson Coefficients from Table 1, one then predicts:

$$\text{Re}(A_2)^{\text{th}} = (0.82 \pm 0.33) \cdot 10^{-8} \text{ GeV}, \quad (108)$$

in reasonable agreement with the experimental value $\text{Re}(A_2)^{\text{exp}} = 1.210(2) \cdot 10^{-8} \text{ GeV}$ [6]. The measured value of A_2 is of course exactly reproduced, taking instead as input the phenomenological determination of $a_{27}(\mu_0)$ in Eq. (54).

From the measured τ spectral functions, we have been able to determine $F^2 a_{88}^{\lambda\lambda}(m_\tau)$ in Eq. (93), which allows us to predict the $K \rightarrow \pi\pi$ matrix elements of the operator Q_8 . Safely neglecting the very suppressed $a_{88}^{\delta\delta}$ contribution, we find at $\mu_0 = 1 \text{ GeV}$:

$$\begin{aligned} \langle Q_8(\mu_0) \rangle_0 &= 1.62 (45)_{a_{88}^{\lambda\lambda}}(10)_{\Delta_L}(6)_{\Delta_C}, \\ \langle Q_8(\mu_0) \rangle_2 &= 0.37 (10)_{a_{88}^{\lambda\lambda}}(6)_{\Delta_L}(3)_{\Delta_C}. \end{aligned} \quad (109)$$

The isotensor matrix element governs the SM contribution to the CP-violating ratio ε'/ε associated with the ($I = 2$) electroweak penguin operators [32],

$$(\varepsilon'/\varepsilon)_{\text{EWP}}^{(2)} \equiv \frac{1}{\sqrt{2}|\varepsilon|} \frac{\text{Im}(A_2)^{\text{EWP}}}{\text{Re}(A_0)}, \quad (110)$$

which at $\mu = 1 \text{ GeV}$ is dominated by Q_8 . Taking the experimental values of $\text{Re}(A_0)^{\text{exp}} = 2.704(1) \cdot 10^{-7} \text{ GeV}$ [6] and $|\varepsilon|^{\text{exp}} = 2.228(11) \cdot 10^{-3}$ [94], and

$$\text{Im}(A_2)_{Q_8}^{\text{EWP}} = G \text{Im}[C_8(\mu)] \langle Q_8(\mu) \rangle_2, \quad (111)$$

one finds

$$(\varepsilon'/\varepsilon)_{\text{EWP},Q_8}^{(2)} = \left(-5.6 \pm 1.5_{a_{88}^{\lambda\lambda}} \pm 0.9_{\Delta_L} \pm 0.5_{\Delta_C} \right) \cdot 10^{-4} = (-5.6 \pm 1.8) \cdot 10^{-4}. \quad (112)$$

On the other hand, using Eq. (106) the (smaller) $Q_{9,10}$ contribution is simply given by

$$(\varepsilon'/\varepsilon)_{\text{EWP},Q_{9,10}}^{(2)} = \frac{3\omega}{2\sqrt{2}|\varepsilon|} \frac{\text{Im}(C_9 + C_{10})}{\text{Re}(C_1 + C_2)} = (1.1 \pm 0.1) \cdot 10^{-4}, \quad (113)$$

where the ratio $\omega \equiv \text{Re}A_2/\text{Re}A_0 = 0.0447(1)$ has been taken from experimental data. Adding this contribution one finally finds

$$(\varepsilon'/\varepsilon)_{\text{EWP}}^{(2)} = \left(-4.5 \pm 1.5_{a_{88}^{\lambda\lambda}} \pm 0.9_{\Delta_L} \pm 0.5_{\Delta_C} \right) \cdot 10^{-4} = (-4.5 \pm 1.8) \cdot 10^{-4}. \quad (114)$$

This result agrees very well with the value $-(3.5 \pm 2.2) \cdot 10^{-4}$, obtained in Refs. [32, 33] with a large- N_C estimate of $a_{88}^{\lambda\lambda}$ (as well as the smaller contributions of the other couplings),¹⁶ instead of our determination from τ decay data.

¹⁶We thank Hector Gisbert for cross-checking this number.

6.1 Fit to lattice data

Our NLO results for the kaon decay amplitudes allow us to perform a direct fit to the lattice data of the RBC-UKQCD collaboration [7]. The numerical values for the matrix elements of the different four-quark operators provided in Ref. [7] can be fitted to our analytic expressions in Eqs. (102), (103), (105) and (106). In Ref. [7], the ten $I = 0$ matrix elements are given at $\mu = 4 \text{ GeV}$ in the $\overline{\text{MS}}$ scheme, together with their statistical covariance matrix.¹⁷ Systematic uncertainties are estimated to be a 15.7%. We run those matrix elements to $\mu = 1 \text{ GeV}$, propagating their uncertainties, and use afterwards the relations (105) to reduce the operator basis to the seven independent $I = 0$ operators. The matrix elements of the three independent (in the isospin limit) $I = 2$ operators can also be found in Ref. [7] (see also Refs. [34] and [35]).

The fitted results for our seven $a_i(\mu)$ parameters are displayed in Table 5. The fit returns a relatively small p -value ($p = 8\%$), which mainly arises from a small tension between $\langle Q_8 \rangle_0$ and $\langle Q_8 \rangle_2$ (the lattice determination of $\langle Q_8 \rangle_0$ favours smaller values for $|a_{88}^{\lambda\lambda}|$ than $\langle Q_8 \rangle_2$). The fitted parameters are in good agreement with the phenomenological values of a_{27} and $F^2 a_{88}^{\lambda\lambda}$ found in the previous sections, which are shown in the second line of the table. The third line collects the predicted numerical values for those couplings in the large- N_C limit, given in Section 2.4. This limit is able to correctly reproduce the hierarchy of the couplings, with the exception of a_{27} and, especially, a_8^A . Notice also the large error in the fitted value of the coupling $a_8^S(\mu_0)$ that governs the contribution of the operator $Q_+ \equiv Q_2 + Q_1$ to the isoscalar $K \rightarrow \pi\pi$ amplitude. With the current precision, the lattice data are still insensitive to this parameter because its contribution to g_8 in Eq. (42) is suppressed by a factor 1/10.

	$a_{27}(\mu_0)$	$a_8^S(\mu_0)$	$a_8^A(\mu_0)$	$a_{LR}^{\delta\delta}(\mu_0)$	$a_{LR}^{\lambda\lambda}(\mu_0)$	$F^2 a_{88}^{\delta\delta}(\mu_0)$	$F^2 a_{88}^{\lambda\lambda}(\mu_0)$
Lattice	0.64 (10)	-0.2 (24)	2.7 (5)	-0.48 (41)	-1.17 (26)	-0.22 (12)	-0.68 (11) GeV^2
K, τ data	0.622 (43)						-0.78 (22) GeV^2
Large N_C	1	1	1	0	-1.06	0	-0.70 GeV^2

Table 5: Values at $\mu_0 = 1 \text{ GeV}$ ($\overline{\text{MS}}$ -NDR) of the $a_i(\mu_0)$ parameters, extracted from a NLO fit to the lattice data (first line) and from experimental data (second line), compared with their large- N_C predictions (third line).

From the measured $K \rightarrow \pi\pi$ rates, it is not possible to extract separate values for the different octet couplings. The experimental data only determines the combination g_8 in Eq. (42). Taking into account the absorptive resummation factor Θ_{δ_0} in Eq. (101),¹⁸ one obtains

$$g_8^{\text{exp}} = 3.07 \pm 0.14. \quad (115)$$

¹⁷A useful comparison of the different normalization conventions can be found in Ref. [95].

¹⁸Including only the absorptive one-loop contribution, *i.e.* with $\Theta_{\delta_0} = 1.10$, one gets instead $g_8^{\text{exp}} = 3.60 \pm 0.14$ [33].

Our fit to the lattice data implies $g_8^{\text{Latt}} = 2.6 \pm 0.5$, in good agreement with (115), while the large- N_C determination of the a_i couplings gives a value $g_8^\infty = 1.2 \pm 0.4$ that is clearly too small.

The comparison between the values of the a_i parameters extracted from the lattice data and their large- N_C predictions provides an enlightening anatomy of the well-known $\Delta I = \frac{1}{2}$ rule in non-leptonic kaon decays. The large difference between the isoscalar and isotensor decay amplitudes results from the combination of several interrelated dynamical effects:

1. The table exhibits a large enhancement of $a_8^A(\mu_0)$ by a factor 2.7 that complements the short-distance gluonic enhancement of $C_-(\mu_0) \equiv (C_2 - C_1)(\mu_0)$ at LO [96, 97] and NLO [98–102]. This clearly identifies the main origin of the isoscalar enhancement in the $K \rightarrow \pi\pi$ matrix element of the operator $Q_- \equiv Q_2 - Q_1$, confirming the findings of many previous approaches [20, 23, 103–109].
2. The matrix element of the penguin operator Q_6 receives a chiral enhancement through the factor $8 a_{LR}^{\lambda\lambda}(\mu_0)$. In spite of the small numerical value of the Wilson coefficient $C_6(\mu_0)$, this provides an additional ($\sim 10\%$ at $\mu = 1$ GeV) increment of the $I = 0$ amplitude [110, 111]. Since the anomalous dimension of Q_6 is leading in $1/N_C$, the large- N_C limit is able to capture the chiral enhancement factor, providing a very good approximation to $a_{LR}^{\lambda\lambda}(\mu_0)$, as exhibited in Table 5. However, this is not enough to reproduce the physical hadronic matrix element of Q_6 [31]. One still needs to incorporate the very sizeable corrections from χ PT loops [92].
3. The χ PT loop contributions are subleading in the $1/N_C$ counting but they are enhanced by large infrared logarithms and, moreover, contain very important unitarity corrections associated with the final-state interactions of the emerging pions [92]. As shown in Table 3, the one-loop χ PT correction provides a sizeable 30% enhancement of the isoscalar amplitude [21, 48, 92, 112] that is further reinforced by the all-order resummation of absorptive contributions through the factor Θ_{δ_0} in Eq. (101). The corresponding χ PT corrections on $\text{Re}(A_2)$ are very mild.
4. In addition, there is a sizeable suppression of $a_{27}(\mu_0)$ by about 30–40%, with respect to its expected value at $N_C \rightarrow \infty$, which implies a corresponding suppression of the amplitude A_2 . This effect was suggested long time ago through a large- N_C topological analysis of the $K \rightarrow \pi\pi$ amplitudes [23], showing that the leading and subleading contributions in $1/N_C$ (excluding penguins) appear anticorrelated in g_8 and g_{27} , so that the enhancement of one coupling requires the suppression of the other.¹⁹ The anticorrelation of the two colour structures has been numerically confirmed by the RBC-UKQCD lattice evaluation of A_2 [113], and corroborated by a more recent lattice analysis of the scaling with N_C of the $K \rightarrow \pi$ amplitudes in a simplified setting with four degenerate quark flavours ($m_u = m_d = m_s = m_c$) [114, 115].

¹⁹At LO, the topological parameters a, b, c defined in Ref. [23] can be easily related to our $a_i(\mu)$ couplings: $a + b = a_{27}(C_1 + C_2)$, $b \approx \frac{1}{2} a_8^A(C_1 - C_2 + C_3) + \frac{1}{10} (6 a_{27} - a_8^S)(C_1 + C_2) - \frac{1}{2} a_8^S C_3$ and $c \approx 8 a_{LR}^{\lambda\lambda} C_6 + \frac{1}{2} (a_8^A + a_8^S) C_4$. They are also directly related to the lattice topologies discussed in Ref. [113].

It is worth mentioning at this point that these dynamical features are fully supported at the inclusive level by the NLO calculation of the two-point correlation function (without electroweak penguin operators)

$$\Psi(q^2) \equiv \int d^4x e^{iqx} \langle 0|T(\mathcal{L}^{\Delta S=1}(x) \mathcal{L}^{\Delta S=1}(0)^\dagger)|0\rangle = G^2 \sum_{i,j=1}^6 C_i(\mu) C_j(\mu)^* \psi_{ij}(q^2), \quad (116)$$

presented in Refs. [20, 23, 116, 117]. This correlator does not involve any hadronic state and, therefore, can be rigorously analyzed with short-distance QCD methods. In order to better visualise the large impact of gluonic corrections, it is convenient to simplify the discussion and restrict ourselves to the non-penguin operators Q_\pm . In the absence of penguin-like contributions, these two operators are multiplicatively renormalizable, which allows one to derive compact analytical expressions for the spectral functions associated with the $C_\pm(\mu) Q_\pm$ terms (exact numerical results for the full correlator can be found in Ref. [117]):

$$\begin{aligned} \rho_\pm(t) &\equiv \frac{1}{\pi} \text{Im} \Psi_{\pm\pm}(t) \\ &= \theta(t) \frac{2}{45} G^2 C_\pm^2(M_W^2) N_C^2 \left(1 \pm \frac{1}{N_C}\right) \frac{t^4}{(4\pi)^6} \alpha_s(t)^{-2\hat{\gamma}_\pm} \left[1 + \zeta_\pm \frac{\alpha_s(t)}{\pi}\right], \end{aligned} \quad (117)$$

where the $\frac{1}{N_C}$ -suppressed powers $\hat{\gamma}_\pm = \gamma_\pm^{(1)}/\beta_1 = \pm \frac{9}{11N_C} (1 \mp \frac{1}{N_C}) / (1 - \frac{6}{11N_C})$ contain the LO anomalous dimensions that enhance the Wilson coefficient $C_-(\mu)$ ($\hat{\gamma}_- = -\frac{4}{9}$) and suppress $C_+(\mu)$ ($\hat{\gamma}_+ = +\frac{2}{9}$). Since $\Psi(t)$ is a renormalization-invariant quantity, the logarithmic α_s corrections have been already reabsorbed with the choice $\mu^2 = t$. At this level of approximation ($\zeta_\pm = 0$), it is impossible to understand the big ratio A_0/A_2 (or, equivalently, g_8/g_{27}) with the information provided by the spectral functions $\rho_\pm(t)$ [18, 118]. The physics picture gets completely changed once the NLO corrections are included: $\rho_-(t)$ gets a huge enhancement through the positive NLO correction $\zeta_- = \frac{9139}{810}$, while the corresponding correction to $\rho_+(t)$ is negative and 6 times smaller, $\zeta_+ = -\frac{3649}{1620}$ [23, 117]. In both cases, the NLO short-distance Wilson coefficients only contribute a small part of the ζ_\pm corrections (17% and 8%, respectively, for ζ_- and ζ_+). More interesting, this enhancement/suppression pattern completely disappears in the large- N_C limit where $\zeta_+^\infty = \zeta_-^\infty = \frac{9}{4}$ [116].

Since Q_6 is the only operator (excluding electroweak penguins) with a non-vanishing anomalous dimension at $N_C \rightarrow \infty$, it is possible to make an analogous computation of $\rho_6(t) \equiv \frac{1}{\pi} \text{Im} \Psi_{66}(t)$ in the large- N_C limit [116]. The result is in fact known to NNLO [20]:

$$\rho_6(t) = \theta(t) \frac{12}{5} G^2 |C_6(M_W^2)|^2 \frac{t^4}{(4\pi)^6} \alpha_s(t)^{18/11} \left[1 + \frac{117501}{4840} \frac{\alpha_s(t)}{\pi} + 470.72 \left(\frac{\alpha_s(t)}{\pi}\right)^2\right]. \quad (118)$$

This exhibits again a huge dynamical enhancement which persists at higher perturbative orders, but this time the enhancement is already captured in the large- N_C limit. The NLO Wilson coefficient only contributes a 13% of the non-logarithmic $\mathcal{O}(\alpha_s)$ correction.

6.2 F_π determination from inclusive τ -decay data

Instead of determining $a_{88}^{\lambda\lambda}$ from τ decays, we can use the value extracted from our fit to the lattice data of the RBC-UKQCD collaboration. Since we have also fitted $a_{88}^{\delta\delta}$, we can obtain the full dimension-six contribution to the OPE of $\Pi_{V-A}^d(s)$, at NLO in both α_s and the χ PT expansion. Taking into account the complete scale dependence of $\langle \mathcal{O}_{6,V-A}^d(\mu) \rangle$ in Eq. (82), the dispersion relation of Eq. (88) for the weight $\hat{\omega}(s) = (1 - s/s_0)^2$ generalizes, up to corrections suppressed by α_s and 8 powers of the energy scale, to

$$\int_{s_{\text{th}}}^{s_0} \frac{ds}{s_0} \left(1 - \frac{s}{s_0}\right)^2 \frac{1}{\pi} \text{Im} \Pi_{V-A}(s) - \frac{\langle \mathcal{O}_{6,V-A}^d(s_0) \rangle'}{s_0^3} + \delta_{\text{DV}}[\hat{\omega}(s), s_0] = 2 \frac{F_\pi^2}{s_0} \left(1 - \frac{M_\pi^2}{s_0}\right)^2, \quad (119)$$

where $\langle \mathcal{O}_{6,V-A}^d(s_0) \rangle'$ equals $\langle \mathcal{O}_{6,V-A}^d(s_0) \rangle$ in Eq. (82), with the changes $A_{1,8} \rightarrow A_{1,8} + \frac{3}{2} B_{1,8}$ and $B_{1,8} \rightarrow 0$. In Table 5, the parameters $a_{88}^{\lambda\lambda}(\mu)$ and $a_{88}^{\delta\delta}(\mu)$ have been determined at $\mu = 1 \text{ GeV}$. Their running up to s_0 is governed by the known μ dependence of Q_7 and Q_8 at NLO because the χ PT coupling $e^2 g_8 g_{\text{ewk}}$ in Eq. (43) does not depend on the short-distance renormalization scale. At $s_0 = m_\tau^2$ one finds:

$$\langle \mathcal{O}_{6,V-A}^d(m_\tau^2) \rangle' = -(2.9 \pm 0.5) \cdot 10^{-3} \text{ GeV}. \quad (120)$$

The negligible role of duality violations for this weight function at $s_0 \sim m_\tau^2$, together with the good knowledge of the very small power corrections involved, translate into a very powerful prediction for its associated integral. In Fig. 7 we display the s_0 dependence of

$$F_{V\pm A}^{(2)}(s_0) \equiv \int_{s_{\text{th}}}^{s_0} \frac{ds}{s_0} \left(1 - \frac{s}{s_0}\right)^2 \frac{1}{\pi} \text{Im} \Pi_{V\pm A}(s) \pm 2 \frac{F_\pi^2}{s_0} \left(1 - \frac{M_\pi^2}{s_0}\right)^2 - \frac{\langle \mathcal{O}_{6,V\pm A}^d(s_0) \rangle'}{s_0^3}. \quad (121)$$

Similarly to what we did before in Fig. 3 with the weight $(1 - s/s_0)$, we plot also the corresponding $V + A$ integral, although neglecting in that case the relatively very small contribution from $\langle \mathcal{O}_{6,V+A}^d \rangle'$ that is irrelevant for the comparison. For the $V - A$ distribution, we have used the value of $\langle \mathcal{O}_{6,V-A}^d(m_\tau^2) \rangle'$ in Eq. (120), running it down to every s_0 at NLO in QCD. Above 2 GeV^2 , one observes an exact cancellation of the vector and axial-vector contributions to $F_{V-A}^{(2)}(s_0)$, which remains compatible with zero within 1σ , even when the experimental data are precise enough to resolve the predicted zero of $F_{V-A}^{(2)}(s_0)$ with a $\sim 0.5\%$ accuracy with respect to the normalization of the total $V + A$ distribution.

Since the strong cancellation involves the pion decay constant, one can exploit the theoretical prediction $F_{V-A}^{(2)}(s_0 \sim m_\tau^2) = 0$ to determine F_π . Although the pion contribution in Eq. (121) is suppressed by two powers of energy, the sensitivity is good enough to derive a precise value for F_π :

$$F_\pi^{\text{incl}} = (92.6 \pm 0.6) \text{ MeV}, \quad \sqrt{2} F_\pi^{\text{incl}} = (130.9 \pm 0.8) \text{ MeV}, \quad (122)$$

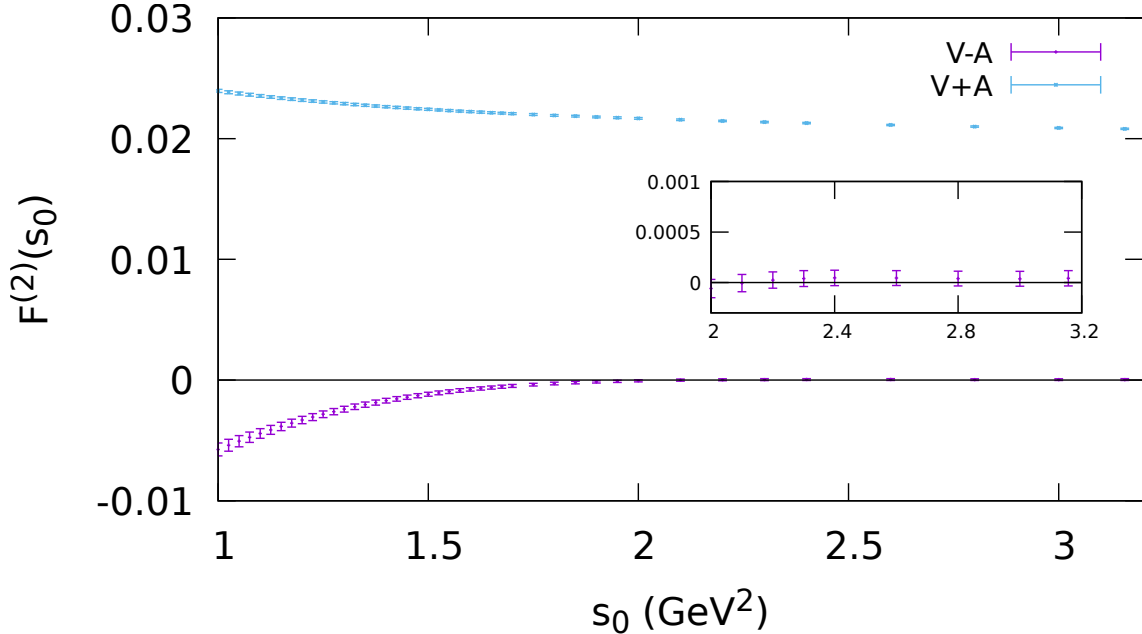


Figure 7: $F_{V\pm A}^{(2)}(s_0)$ as defined in Eq. (121). The error bars include the experimental uncertainties and the theoretical errors associated with $\langle \mathcal{O}_{6,V-A}^d \rangle'$.

in perfect agreement with the values found in the literature from other sectors [94, 119]. Notice that we have not used any information from the decay $\tau^- \rightarrow \pi^- \nu_\tau$.

Another possible application of this result is reinterpreting it as a powerful constraint on hypothetical new physics contributions that do not respect chiral symmetry at short distances. Contributions of this type would easily spoil the strong cancellation between the vector and axial-vector integrated distributions, in disagreement with the behaviour displayed in Fig. 7. This idea was already exploited in Ref. [120], where powerful bounds on new physics above the TeV scale were extracted.

Finally, we can also estimate the dimension-8 condensate, using the triple-pinned dispersion relation

$$\int_{s_{th}}^{s_0} \frac{ds}{s_0} \left(1 - \frac{s}{s_0}\right)^3 \frac{1}{\pi} \text{Im}\Pi_{V-A}(s) - 2 \frac{F_\pi^2}{s_0} \left(1 - \frac{m_\pi^2}{s_0}\right)^3 - 3 \frac{\langle \mathcal{O}_{6,V-A}^d(s_0) \rangle''}{s_0^3} - \frac{\langle \mathcal{O}_{8,V-A}^d \rangle}{s_0^4} = 0, \quad (123)$$

where now $\langle \mathcal{O}_{6,V-A}^d(s_0) \rangle''$ equals $\langle \mathcal{O}_{6,V-A}^d(s_0) \rangle$ in Eq. (82), with the changes $A_{1,8} \rightarrow A_{1,8} + \frac{1}{2} B_{1,8}$ and $B_{1,8} \rightarrow 0$, and the equality holds up to very tiny logarithmic (α_s -suppressed) corrections to $D \geq 8$ and duality violations. Since $\langle \mathcal{O}_{6,V-A}^d(s_0) \rangle''$ is determined by our lattice fit, the τ data now implies:

$$\langle \mathcal{O}_{8,V-A}^d \rangle = (-1.3 \pm 0.7) \cdot 10^{-2} \text{ GeV}^8, \quad (124)$$

which is in good agreement with the different determinations found in the literature [81, 86].

7 Conclusions

We have presented a detailed analysis of light-quark four-fermion operators, using the symmetry relations emerging from their chiral $SU(3)_L \otimes SU(3)_R$ structure and a low-energy effective Lagrangian approach. This has allowed us to derive rigorous relations between non-perturbative parameters appearing in different physical processes. In particular, we have studied in a systematic way the relations between the dimension-six vacuum condensates entering the OPE of the vector and axial-vector QCD currents, and the hadronic matrix elements of weak operators in $\Delta S = 1$ ($K \rightarrow \pi\pi$) and $\Delta S = 2$ ($K^0 - \bar{K}^0$) transitions. The χ PT framework provides a powerful way to determine the low-energy realization of the four-quark operators, taking into account their different decomposition in irreducible representations of the chiral group and ordering their phenomenological impact through the chiral momentum expansion. The non-trivial dynamical information gets encoded in a few low-energy constants that characterize the different structures allowed by symmetry. These constants can be easily estimated in the limit of a large number of QCD colours, which provides useful reference values to compare with.

As a first important phenomenological application, we have determined the electromagnetic penguin contribution to the ratio ε'/ε , which parametrizes the direct violation of CP symmetry in the $K \rightarrow \pi\pi$ amplitudes. The relevant operator has an (88) structure that gives rise to a leading $\mathcal{O}(p^0)$ contribution, providing a sizeable chiral enhancement of its matrix elements. The symmetry relations connect this $\mathcal{O}(p^0)$ term with the vacuum matrix element of the corresponding four-quark operator appearing in the OPE of the Π_{V-A}^d correlator, which is accessible through hadronic τ decay data. Using the measured invariant-mass distribution of the final hadrons in τ decays, we have found

$$(\varepsilon'/\varepsilon)_{\text{EWP}}^{(2)} = -(4.5 \pm 1.8) \cdot 10^{-4}, \quad (125)$$

at NLO in χ PT. This phenomenological determination is in excellent agreement with the values obtained in the χ PT calculation of Refs. [32, 33], with a large- N_C estimate of $a_{88}^{\lambda\lambda}$, and with the most recent lattice results [7].

Combining our analytical evaluation of the $K \rightarrow \pi\pi$ matrix elements [32, 33], at NLO in χ PT, with the numerical analysis of the RBC-UKQCD collaboration [7], we have extracted the leading chiral couplings through a direct fit to the lattice data. The comparison of these results, shown in Table 5, with the corresponding large- N_C estimates provides an enlightening anatomy of the well-known enhancement of the isoscalar $K \rightarrow \pi\pi$ amplitude, which we have discussed in detail in Section 6.1. A dynamical QCD understanding of the so-called $\Delta I = \frac{1}{2}$ rule clearly emerges from this exercise.

The comparison with the lattice results also confirms that the $K \rightarrow \pi\pi$ matrix elements of the penguin operators Q_6 and Q_8 are well approximated by the large- N_C limit, once the large χ PT loop corrections (subleading in $1/N_C$) are properly taken into account. This

was suggested long time ago [48, 92], based on the fact that the anomalous dimensions of these two operators are leading in $1/N_C$ and, moreover, the large- N_C limit gives a good estimate of their exact values. The numerical confirmation of this property further reinforces the theoretical accuracy of the updated Standard Model prediction of ε'/ε presented in Refs. [32, 33], since Q_6 and Q_8 completely dominate the quantitative evaluation of this important observable.

Finally, we have also presented a beautiful consistency test between the experimental τ -decay distribution, the χ PT analytical description and the numerical lattice data. Using the lattice fit to determine the dimension-six condensate contribution to the Π_{V-A}^d correlator, we have extracted the pion decay constant from the integrated $V - A$ invariant-mass distribution of the final hadrons in inclusive τ decays. The resulting value, given in Eq. (122), is surprisingly accurate and in excellent agreement with the direct determinations from $\pi \rightarrow \mu\nu$ [94] and from lattice simulations [119].

Acknowledgements

We are grateful to Hans Bijnens, Vincenzo Cirigliano, Hector Gisbert and Chris Sachrajda for useful discussions. This work is partially supported by the Agence Nationale de la Recherche (ANR) under grant ANR-19-CE31-0012 (project MORA), by the Spanish Government and ERDF funds from the European Commission (FPA2017-84445-P), by the Generalitat Valenciana (PROMETEO/2017/053), by the EU H2020 research and innovation programme (Grant Agreement 824093) and by the EU COST Action CA16201 PARTICLEFACE.

References

- [1] Kenneth G. Wilson. Nonlagrangian models of current algebra. *Phys. Rev.*, 179: 1499–1512, 1969. doi: 10.1103/PhysRev.179.1499.
- [2] Gerhard Buchalla, Andrzej J. Buras, and Markus E. Lautenbacher. Weak decays beyond leading logarithms. *Rev. Mod. Phys.*, 68:1125–1144, 1996. doi: 10.1103/RevModPhys.68.1125.
- [3] Antonio Pich. Effective field theory: Course. In *Les Houches Summer School in Theoretical Physics, Session 68: Probing the Standard Model of Particle Interactions*, pages 949–1049, 6 1998.
- [4] Aneesh V. Manohar. Introduction to Effective Field Theories. *Les Houches Lect. Notes*, 108, 2020. doi: 10.1093/oso/9780198855743.003.0002.
- [5] Matthias Neubert. Renormalization Theory and Effective Field Theories. *Les Houches Lect. Notes*, 108, 2020. doi: 10.1093/oso/9780198855743.003.0001.

- [6] Vincenzo Cirigliano, Gerhard Ecker, Helmut Neufeld, Antonio Pich, and Jorge Portoles. Kaon Decays in the Standard Model. *Rev. Mod. Phys.*, 84:399, 2012. doi: 10.1103/RevModPhys.84.399.
- [7] R. Abbott et al. Direct CP violation and the $\Delta I = 1/2$ rule in $K \rightarrow \pi\pi$ decay from the standard model. *Phys. Rev. D*, 102(5):054509, 2020. doi: 10.1103/PhysRevD.102.054509.
- [8] Antonio Pich. Precision physics with inclusive QCD processes. *Prog. Part. Nucl. Phys.*, 117:103846, 2021. doi: 10.1016/j.ppnp.2020.103846.
- [9] Gunnar Kallen. On the definition of the Renormalization Constants in Quantum Electrodynamics. *Helv. Phys. Acta*, 25(4):417, 1952. doi: 10.1007/978-3-319-00627-7_90.
- [10] H. Lehmann. On the Properties of propagation functions and renormalization constants of quantized fields. *Nuovo Cim.*, 11:342–357, 1954. doi: 10.1007/BF02783624.
- [11] E. Braaten, Stephan Narison, and A. Pich. QCD analysis of the tau hadronic width. *Nucl. Phys. B*, 373:581–612, 1992. doi: 10.1016/0550-3213(92)90267-F.
- [12] Mikhail A. Shifman, A.I. Vainshtein, and Valentin I. Zakharov. QCD and Resonance Physics. Theoretical Foundations. *Nucl. Phys. B*, 147:385–447, 1979. doi: 10.1016/0550-3213(79)90022-1.
- [13] John F. Donoghue, Eugene Golowich, and Barry R. Holstein. The $\Delta S = 2$ Matrix Element for $K^0 - \bar{K}^0$ Mixing. *Phys. Lett. B*, 119:412, 1982. doi: 10.1016/0370-2693(82)90702-X.
- [14] Johan Bijnens, Hidenori Sonoda, and Mark B. Wise. On the Validity of Chiral Perturbation Theory for $K^0 - \bar{K}^0$ Mixing. *Phys. Rev. Lett.*, 53:2367, 1984. doi: 10.1103/PhysRevLett.53.2367.
- [15] A. Pich and E. De Rafael. $K - \bar{K}$ Mixing in the Standard Model. *Phys. Lett. B*, 158:477–484, 1985. doi: 10.1016/0370-2693(85)90798-1.
- [16] Claude W. Bernard, Terrence Draper, A. Soni, H. David Politzer, and Mark B. Wise. Application of Chiral Perturbation Theory to $K \rightarrow 2\pi$ Decays. *Phys. Rev. D*, 32:2343–2347, 1985. doi: 10.1103/PhysRevD.32.2343.
- [17] Branko Guberina, Antonio Pich, and Eduardo de Rafael. The Decay $K^+ \rightarrow \pi^+\pi^0$ in the Standard Model. *Phys. Lett. B*, 163:198–202, 1985. doi: 10.1016/0370-2693(85)90220-5.
- [18] Antonio Pich, Branko Guberina, and Eduardo de Rafael. Problem with the $\Delta I = 1/2$ Rule in the Standard Model. *Nucl. Phys. B*, 277:197, 1986. doi: 10.1016/0550-3213(86)90438-4.

- [19] J. Kambor, John H. Missimer, and D. Wyler. The Chiral Loop Expansion of the Nonleptonic Weak Interactions of Mesons. *Nucl. Phys. B*, 346:17–64, 1990. doi: 10.1016/0550-3213(90)90236-7.
- [20] Antonio Pich and Eduardo de Rafael. Four quark operators and nonleptonic weak transitions. *Nucl. Phys. B*, 358:311–382, 1991. doi: 10.1016/0550-3213(91)90351-W.
- [21] J. Kambor, John H. Missimer, and D. Wyler. $K \rightarrow 2\pi$ and $K \rightarrow 3\pi$ decays in next-to-leading order chiral perturbation theory. *Phys. Lett. B*, 261:496–503, 1991. doi: 10.1016/0370-2693(91)90463-Z.
- [22] J. Kambor, John F. Donoghue, Barry R. Holstein, John H. Missimer, and D. Wyler. Chiral symmetry tests in nonleptonic K decay. *Phys. Rev. Lett.*, 68:1818–1821, 1992. doi: 10.1103/PhysRevLett.68.1818.
- [23] Antonio Pich and Eduardo de Rafael. Weak K amplitudes in the chiral and $1/N_C$ expansions. *Phys. Lett. B*, 374:186–192, 1996. doi: 10.1016/0370-2693(96)00171-2.
- [24] Marc Knecht, Santiago Peris, and Eduardo de Rafael. Matrix elements of electroweak penguin operators in the $1/N_C$ expansion. *Phys. Lett. B*, 457:227–235, 1999. doi: 10.1016/S0370-2693(99)00425-6.
- [25] John F. Donoghue and Eugene Golowich. Dispersive calculation of $B_7^{3/2}$ and $B_8^{3/2}$ in the chiral limit. *Phys. Lett. B*, 478:172–184, 2000. doi: 10.1016/S0370-2693(00)00239-2.
- [26] Johan Bijnens, Elvira Gamiz, and Joaquim Prades. Matching the electroweak penguins Q_7 , Q_8 and spectral correlators. *JHEP*, 10:009, 2001. doi: 10.1088/1126-6708/2001/10/009.
- [27] Marc Knecht, Santiago Peris, and Eduardo de Rafael. A critical reassessment of Q_7 and Q_8 matrix elements. *Phys. Lett. B*, 508:117–126, 2001. doi: 10.1016/S0370-2693(01)00420-8.
- [28] Vincenzo Cirigliano, John F. Donoghue, Eugene Golowich, and Kim Maltman. Determination of $\langle(\pi\pi)_{I=2}|\mathcal{Q}_{7,8}|K^0\rangle$ in the chiral limit. *Phys. Lett. B*, 522:245–256, 2001. doi: 10.1016/S0370-2693(01)01250-3.
- [29] Vincenzo Cirigliano, John F. Donoghue, Eugene Golowich, and Kim Maltman. Improved determination of the electroweak penguin contribution to ϵ'/ϵ in the chiral limit. *Phys. Lett. B*, 555:71–82, 2003. doi: 10.1016/S0370-2693(03)00010-8.
- [30] O. Cata and S. Peris. Long distance dimension eight operators in B_K . *JHEP*, 03:060, 2003. doi: 10.1088/1126-6708/2003/03/060.
- [31] Thomas Hambye, Santiago Peris, and Eduardo de Rafael. $\Delta I = 1/2$ and ϵ'/ϵ in large- N_c QCD. *JHEP*, 05:027, 2003. doi: 10.1088/1126-6708/2003/05/027.

- [32] Hector Gisbert and Antonio Pich. Direct CP violation in $K^0 \rightarrow \pi\pi$: Standard Model Status. *Rept. Prog. Phys.*, 81(7):076201, 2018. doi: 10.1088/1361-6633/aac18e.
- [33] V. Cirigliano, H. Gisbert, A. Pich, and A. Rodríguez-Sánchez. Isospin-violating contributions to ϵ'/ϵ . *JHEP*, 02:032, 2020. doi: 10.1007/JHEP02(2020)032.
- [34] T. Blum et al. $K \rightarrow \pi\pi$ $\Delta I = 3/2$ decay amplitude in the continuum limit. *Phys. Rev. D*, 91(7):074502, 2015. doi: 10.1103/PhysRevD.91.074502.
- [35] T. Blum et al. Lattice determination of the $K \rightarrow (\pi\pi)_{I=2}$ Decay Amplitude A_2 . *Phys. Rev. D*, 86:074513, 2012. doi: 10.1103/PhysRevD.86.074513.
- [36] Antonio Pich. Effective Field Theory with Nambu-Goldstone Modes. *Les Houches Lect. Notes*, 108, 2020. doi: 10.1093/oso/9780198855743.003.0003.
- [37] J. Gasser and H. Leutwyler. Chiral Perturbation Theory: Expansions in the Mass of the Strange Quark. *Nucl. Phys. B*, 250:465–516, 1985. doi: 10.1016/0550-3213(85)90492-4.
- [38] A. Pich. Chiral perturbation theory. *Rept. Prog. Phys.*, 58:563–610, 1995. doi: 10.1088/0034-4885/58/6/001.
- [39] Steven Weinberg. Phenomenological Lagrangians. *Physica A*, 96(1-2):327–340, 1979. doi: 10.1016/0378-4371(79)90223-1.
- [40] Christoph Lehner and Christian Sturm. Matching factors for $\Delta S = 1$ four-quark operators in RI/SMOM schemes. *Phys. Rev. D*, 84:014001, 2011. doi: 10.1103/PhysRevD.84.014001.
- [41] G. Ecker, J. Gasser, A. Pich, and E. de Rafael. The Role of Resonances in Chiral Perturbation Theory. *Nucl. Phys. B*, 321:311–342, 1989. doi: 10.1016/0550-3213(89)90346-5.
- [42] R.J. Crewther. Chiral Reduction of $K \rightarrow 2\pi$ Amplitudes. *Nucl. Phys. B*, 264:277–291, 1986. doi: 10.1016/0550-3213(86)90483-9.
- [43] Frederick J. Gilman and Mark B. Wise. Effective Hamiltonian for $\Delta s = 1$ Weak Nonleptonic Decays in the Six Quark Model. *Phys. Rev. D*, 20:2392, 1979. doi: 10.1103/PhysRevD.20.2392.
- [44] Jeremiah A. Cronin. Phenomenological model of strong and weak interactions in chiral $U(3) \times U(3)$. *Phys. Rev.*, 161:1483–1494, 1967. doi: 10.1103/PhysRev.161.1483.
- [45] Johan Bijnens and Mark B. Wise. Electromagnetic Contribution to ϵ'/ϵ . *Phys. Lett. B*, 137:245–250, 1984. doi: 10.1016/0370-2693(84)90238-7.
- [46] Benjamin Grinstein, Soo-Jong Rey, and Mark B. Wise. CP Violation in Charged Kaon Decay. *Phys. Rev. D*, 33:1495, 1986. doi: 10.1103/PhysRevD.33.1495.

- [47] Andrzej J. Buras, Matthias Jamin, and Markus E. Lautenbacher. The Anatomy of ϵ'/ϵ beyond leading logarithms with improved hadronic matrix elements. *Nucl. Phys. B*, 408:209–285, 1993. doi: 10.1016/0550-3213(93)90535-W.
- [48] E. Pallante, A. Pich, and I. Scimemi. The Standard model prediction for ϵ'/ϵ . *Nucl. Phys. B*, 617:441–474, 2001. doi: 10.1016/S0550-3213(01)00418-7.
- [49] Frederick J. Gilman and Mark B. Wise. $K^0 - \bar{K}^0$ Mixing in the Six Quark Model. *Phys. Rev. D*, 27:1128, 1983. doi: 10.1103/PhysRevD.27.1128.
- [50] Joachim Brod, Martin Gorbahn, and Emmanuel Stamou. Standard-Model Prediction of ϵ_K with Manifest Quark-Mixing Unitarity. *Phys. Rev. Lett.*, 125(17):171803, 2020. doi: 10.1103/PhysRevLett.125.171803.
- [51] Andrzej J. Buras, Matthias Jamin, and Peter H. Weisz. Leading and Next-to-leading QCD Corrections to ϵ Parameter and $B^0 - \bar{B}^0$ Mixing in the Presence of a Heavy Top Quark. *Nucl. Phys. B*, 347:491–536, 1990. doi: 10.1016/0550-3213(90)90373-L.
- [52] Stefan Herrlich and Ulrich Nierste. Enhancement of the $K_L - K_S$ mass difference by short distance QCD corrections beyond leading logarithms. *Nucl. Phys. B*, 419:292–322, 1994. doi: 10.1016/0550-3213(94)90044-2.
- [53] Stefan Herrlich and Ulrich Nierste. The Complete $|\Delta S| = 2$ Hamiltonian in the next-to-leading order. *Nucl. Phys. B*, 476:27–88, 1996. doi: 10.1016/0550-3213(96)00324-0.
- [54] Joachim Brod and Martin Gorbahn. ϵ_K at Next-to-Next-to-Leading Order: The Charm-Top-Quark Contribution. *Phys. Rev. D*, 82:094026, 2010. doi: 10.1103/PhysRevD.82.094026.
- [55] Johan Bijnens, Elvira Gamiz, and Joaquim Prades. The B_K kaon parameter in the chiral limit. *JHEP*, 03:048, 2006. doi: 10.1088/1126-6708/2006/03/048.
- [56] Johan Bijnens and Joaquim Prades. The B_K parameter in the $1/N_C$ expansion. *Nucl. Phys. B*, 444:523–562, 1995. doi: 10.1016/0550-3213(95)00206-8.
- [57] Santiago Peris and Eduardo de Rafael. $K^0 - \bar{K}^0$ mixing in the $1/N_C$ expansion. *Phys. Lett. B*, 490:213–222, 2000. doi: 10.1016/S0370-2693(00)00977-1.
- [58] P. A. Baikov, K. G. Chetyrkin, and Johann H. Kuhn. Order α_s^4 QCD Corrections to Z and τ Decays. *Phys. Rev. Lett.*, 101:012002, 2008. doi: 10.1103/PhysRevLett.101.012002.
- [59] P. A. Baikov, K. G. Chetyrkin, and J. H. Kuhn. Adler Function, Bjorken Sum Rule, and the Crewther Relation to Order α_s^4 in a General Gauge Theory. *Phys. Rev. Lett.*, 104:132004, 2010. doi: 10.1103/PhysRevLett.104.132004.

- [60] F. Herzog, B. Ruijl, T. Ueda, J. A. M. Vermaseren, and A. Vogt. On Higgs decays to hadrons and the R-ratio at N⁴LO. *JHEP*, 08:113, 2017. doi: 10.1007/JHEP08(2017)113.
- [61] P. A. Baikov, K. G. Chetyrkin, J. H. Kuhn, and J. Rittinger. Adler Function, Sum Rules and Crewther Relation of Order $\mathcal{O}(\alpha_s^4)$: the Singlet Case. *Phys. Lett. B*, 714: 62–65, 2012. doi: 10.1016/j.physletb.2012.06.052.
- [62] Vincenzo Cirigliano and Eugene Golowich. Analysis of $O(p^2)$ corrections to $\langle \pi\pi|Q_{7,8}|K \rangle$. *Phys. Lett. B*, 475:351–360, 2000. doi: 10.1016/S0370-2693(00)00098-8.
- [63] L.V. Lanin, V.P. Spiridonov, and K.G. Chetyrkin. Contribution of Four Quark Condensates to Sum Rules for ρ and A1 Mesons. (In Russian). *Yad. Fiz.*, 44:1372–1374, 1986.
- [64] L.E. Adam and K.G. Chetyrkin. Renormalization of four quark operators and QCD sum rules. *Phys. Lett. B*, 329:129–135, 1994. doi: 10.1016/0370-2693(94)90528-2.
- [65] Diogo Boito, Dirk Hornung, and Matthias Jamin. Anomalous dimensions of four-quark operators and renormalon structure of mesonic two-point correlators. *JHEP*, 12:090, 2015. doi: 10.1007/JHEP12(2015)090.
- [66] C. Vafa and Edward Witten. Restrictions on Symmetry Breaking in Vector-Like Gauge Theories. *Nucl. Phys. B*, 234:173–188, 1984. doi: 10.1016/0550-3213(84)90230-X.
- [67] W.J. Marciano and A. Sirlin. Electroweak Radiative Corrections to tau Decay. *Phys. Rev. Lett.*, 61:1815–1818, 1988. doi: 10.1103/PhysRevLett.61.1815.
- [68] Eric Braaten and Chong-Sheng Li. Electroweak radiative corrections to the semi-hadronic decay rate of the tau lepton. *Phys. Rev. D*, 42:3888–3891, 1990. doi: 10.1103/PhysRevD.42.3888.
- [69] Jens Erler. Electroweak radiative corrections to semileptonic tau decays. *Rev. Mex. Fis.*, 50:200–202, 2004.
- [70] Michel Davier, Andreas Höcker, Bogdan Malaescu, Chang-Zheng Yuan, and Zhiqing Zhang. Update of the ALEPH non-strange spectral functions from hadronic τ decays. *Eur. Phys. J. C*, 74(3):2803, 2014. doi: 10.1140/epjc/s10052-014-2803-9.
- [71] F. Le Diberder and A. Pich. Testing QCD with τ decays. *Phys. Lett. B*, 289:165–175, 1992. doi: 10.1016/0370-2693(92)91380-R.
- [72] M.S. Dubovikov and Andrei V. Smilga. On nonperturbative qcd effects in imaginary part of polarization operator of quark and gluon currents (in Russian). *Yad. Fiz.*, 37:984–992, 1983.

- [73] Boris Chibisov, R.David Dikeman, Mikhail A. Shifman, and N. Uraltsev. Operator product expansion, heavy quarks, QCD duality and its violations. *Int. J. Mod. Phys. A*, 12:2075–2133, 1997. doi: 10.1142/S0217751X97001316.
- [74] Mikhail A. Shifman. Quark hadron duality. In *8th International Symposium on Heavy Flavor Physics*, volume 3, pages 1447–1494, Singapore, 7 2000. World Scientific. doi: 10.1142/9789812810458_0032.
- [75] O. Cata, M. Golterman, and S. Peris. Duality violations and spectral sum rules. *JHEP*, 08:076, 2005. doi: 10.1088/1126-6708/2005/08/076.
- [76] Martin Gonzalez-Alonso, Antonio Pich, and Joaquim Prades. Violation of Quark-Hadron Duality and Spectral Chiral Moments in QCD. *Phys. Rev. D*, 81:074007, 2010. doi: 10.1103/PhysRevD.81.074007.
- [77] Martin Gonzalez-Alonso, Antonio Pich, and Joaquim Prades. Pinched weights and Duality Violation in QCD Sum Rules: a critical analysis. *Phys. Rev. D*, 82:014019, 2010. doi: 10.1103/PhysRevD.82.014019.
- [78] Diogo Boito, Irinel Caprini, Maarten Golterman, Kim Maltman, and Santiago Peris. Hyperasymptotics and quark-hadron duality violations in QCD. *Phys. Rev. D*, 97(5):054007, 2018. doi: 10.1103/PhysRevD.97.054007.
- [79] Diogo Boito, Maarten Golterman, Kim Maltman, James Osborne, and Santiago Peris. Strong coupling from the revised ALEPH data for hadronic τ decays. *Phys. Rev. D*, 91(3):034003, 2015. doi: 10.1103/PhysRevD.91.034003.
- [80] Antonio Pich and Antonio Rodríguez-Sánchez. Determination of the QCD coupling from ALEPH τ decay data. *Phys. Rev. D*, 94(3):034027, 2016. doi: 10.1103/PhysRevD.94.034027.
- [81] Martin González-Alonso, Antonio Pich, and Antonio Rodríguez-Sánchez. Updated determination of chiral couplings and vacuum condensates from hadronic τ decay data. *Phys. Rev. D*, 94(1):014017, 2016. doi: 10.1103/PhysRevD.94.014017.
- [82] Steven Weinberg. Precise relations between the spectra of vector and axial vector mesons. *Phys. Rev. Lett.*, 18:507–509, 1967. doi: 10.1103/PhysRevLett.18.507.
- [83] B. Blok, Mikhail A. Shifman, and Da-Xin Zhang. An Illustrative example of how quark hadron duality might work. *Phys. Rev. D*, 57:2691–2700, 1998. doi: 10.1103/PhysRevD.57.2691. [Erratum: *Phys.Rev.D* 59, 019901 (1999)].
- [84] Mikhail A. Shifman. Snapshots of hadrons or the story of how the vacuum medium determines the properties of the classical mesons which are produced, live and die in the QCD vacuum. *Prog. Theor. Phys. Suppl.*, 131:1–71, 1998. doi: 10.1143/PTPS.131.1.

- [85] Oscar Cata, Maarten Golterman, and Santi Peris. Unraveling duality violations in hadronic tau decays. *Phys. Rev. D*, 77:093006, 2008. doi: 10.1103/PhysRevD.77.093006.
- [86] Diogo Boito, Anthony Francis, Maarten Golterman, Renwick Hudspith, Randy Lewis, Kim Maltman, and Santiago Peris. Low-energy constants and condensates from ALEPH hadronic τ decay data. *Phys. Rev. D*, 92(11):114501, 2015. doi: 10.1103/PhysRevD.92.114501.
- [87] V. Cirigliano, G. Ecker, H. Neufeld, and A. Pich. Isospin breaking in $K \rightarrow \pi\pi$ decays. *Eur. Phys. J. C*, 33:369–396, 2004. doi: 10.1140/epjc/s2003-01579-3.
- [88] Johan Bijnens and Joaquim Prades. ϵ'_K/ϵ_K in the chiral limit. *JHEP*, 06:035, 2000. doi: 10.1088/1126-6708/2000/06/035.
- [89] Stephan Narison. New QCD estimate of the kaon penguin matrix elements and ϵ'/ϵ . *Nucl. Phys. B*, 593:3–30, 2001. doi: 10.1016/S0550-3213(00)00618-0.
- [90] G. Ecker, J. Kambor, and D. Wyler. Resonances in the weak chiral Lagrangian. *Nucl. Phys. B*, 394:101–138, 1993. doi: 10.1016/0550-3213(93)90103-V.
- [91] G. Ecker, G. Isidori, G. Muller, H. Neufeld, and A. Pich. Electromagnetism in nonleptonic weak interactions. *Nucl. Phys. B*, 591:419–434, 2000. doi: 10.1016/S0550-3213(00)00568-X.
- [92] Elisabetta Pallante and Antonio Pich. Strong enhancement of ϵ'/ϵ through final state interactions. *Phys. Rev. Lett.*, 84:2568–2571, 2000. doi: 10.1103/PhysRevLett.84.2568.
- [93] G. Colangelo, J. Gasser, and H. Leutwyler. $\pi\pi$ scattering. *Nucl. Phys. B*, 603:125–179, 2001. doi: 10.1016/S0550-3213(01)00147-X.
- [94] P.A. Zyla et al. Review of Particle Physics. *PTEP*, 2020(8):083C01, 2020. doi: 10.1093/ptep/ptaa104.
- [95] Jason Aebischer, Christoph Bobeth, and Andrzej J. Buras. ϵ'/ϵ in the Standard Model at the Dawn of the 2020s. *Eur. Phys. J. C*, 80(8):705, 2020. doi: 10.1140/epjc/s10052-020-8267-1.
- [96] Guido Altarelli and L. Maiani. Octet Enhancement of Nonleptonic Weak Interactions in Asymptotically Free Gauge Theories. *Phys. Lett. B*, 52:351–354, 1974. doi: 10.1016/0370-2693(74)90060-4.
- [97] M. K. Gaillard and Benjamin W. Lee. $\Delta I = 1/2$ Rule for Nonleptonic Decays in Asymptotically Free Field Theories. *Phys. Rev. Lett.*, 33:108, 1974. doi: 10.1103/PhysRevLett.33.108.

- [98] Andrzej J. Buras, Matthias Jamin, M. E. Lautenbacher, and Peter H. Weisz. Effective Hamiltonians for $\Delta S = 1$ and $\Delta B = 1$ nonleptonic decays beyond the leading logarithmic approximation. *Nucl. Phys. B*, 370:69–104, 1992. doi: 10.1016/0550-3213(92)90345-C. [Addendum: Nucl.Phys.B 375, 501 (1992)].
- [99] Andrzej J. Buras, Matthias Jamin, Markus E. Lautenbacher, and Peter H. Weisz. Two loop anomalous dimension matrix for $\Delta S = 1$ weak nonleptonic decays I: $\mathcal{O}(\alpha_s^2)$. *Nucl. Phys. B*, 400:37–74, 1993. doi: 10.1016/0550-3213(93)90397-8.
- [100] Andrzej J. Buras, Matthias Jamin, and Markus E. Lautenbacher. Two loop anomalous dimension matrix for $\Delta S = 1$ weak nonleptonic decays. 2. $\mathcal{O}(\alpha\alpha_s)$. *Nucl. Phys. B*, 400:75–102, 1993. doi: 10.1016/0550-3213(93)90398-9.
- [101] Marco Ciuchini, E. Franco, G. Martinelli, and L. Reina. ϵ'/ϵ at the Next-to-leading order in QCD and QED. *Phys. Lett. B*, 301:263–271, 1993. doi: 10.1016/0370-2693(93)90699-I.
- [102] Marco Ciuchini, E. Franco, G. Martinelli, and L. Reina. The $\Delta S = 1$ effective Hamiltonian including next-to-leading order QCD and QED corrections. *Nucl. Phys. B*, 415:403–462, 1994. doi: 10.1016/0550-3213(94)90118-X.
- [103] William A. Bardeen, A. J. Buras, and J. M. Gerard. A Consistent Analysis of the $\Delta I = 1/2$ Rule for K Decays. *Phys. Lett. B*, 192:138–144, 1987. doi: 10.1016/0370-2693(87)91156-7.
- [104] V. Antonelli, S. Bertolini, M. Fabbrichesi, and E. I. Lashin. The $\Delta I = 1/2$ selection rule. *Nucl. Phys. B*, 469:181–201, 1996. doi: 10.1016/0550-3213(96)00145-9.
- [105] V. Antonelli, S. Bertolini, J. O. Eeg, M. Fabbrichesi, and E. I. Lashin. The $\Delta S = 1$ weak chiral lagrangian as the effective theory of the chiral quark model. *Nucl. Phys. B*, 469:143–180, 1996. doi: 10.1016/0550-3213(96)00144-7.
- [106] S. Bertolini, J. O. Eeg, M. Fabbrichesi, and E. I. Lashin. The $\Delta I = 1/2$ rule and B_K at $\mathcal{O}(p^4)$ in the chiral expansion. *Nucl. Phys. B*, 514:63–92, 1998. doi: 10.1016/S0550-3213(97)00787-6.
- [107] Johan Bijnens and Joaquim Prades. The $\Delta I = 1/2$ rule in the chiral limit. *JHEP*, 01:023, 1999. doi: 10.1088/1126-6708/1999/01/023.
- [108] T. Hambye, G. O. Kohler, and P. H. Soldan. New analysis of the $\Delta I = 1/2$ rule in kaon decays and the \hat{B}_K parameter. *Eur. Phys. J. C*, 10:271–292, 1999. doi: 10.1007/s100529900084.
- [109] Andrzej J. Buras, Jean-Marc Gérard, and William A. Bardeen. Large N Approach to Kaon Decays and Mixing 28 Years Later: $\Delta I = 1/2$ Rule, \hat{B}_K and ΔM_K . *Eur. Phys. J. C*, 74:2871, 2014. doi: 10.1140/epjc/s10052-014-2871-x.

- [110] A. I. Vainshtein, Valentin I. Zakharov, and Mikhail A. Shifman. A Possible mechanism for the $\Delta T = 1/2$ rule in nonleptonic decays of strange particles. *JETP Lett.*, 22:55–56, 1975.
- [111] Mikhail A. Shifman, A. I. Vainshtein, and Valentin I. Zakharov. Light Quarks and the Origin of the $\Delta I = 1/2$ Rule in the Nonleptonic Decays of Strange Particles. *Nucl. Phys. B*, 120:316–324, 1977. doi: 10.1016/0550-3213(77)90046-3.
- [112] Elisabetta Pallante and Antonio Pich. Final state interactions in kaon decays. *Nucl. Phys. B*, 592:294–320, 2001. doi: 10.1016/S0550-3213(00)00601-5.
- [113] P. A. Boyle et al. Emerging understanding of the $\Delta I = 1/2$ Rule from Lattice QCD. *Phys. Rev. Lett.*, 110(15):152001, 2013. doi: 10.1103/PhysRevLett.110.152001.
- [114] A. Donini, P. Hernández, C. Pena, and F. Romero-López. Nonleptonic kaon decays at large N_c . *Phys. Rev. D*, 94(11):114511, 2016. doi: 10.1103/PhysRevD.94.114511.
- [115] Andrea Donini, Pilar Hernández, Carlos Pena, and Fernando Romero-López. Dissecting the $\Delta I = 1/2$ rule at large N_c . *Eur. Phys. J. C*, 80(7):638, 2020. doi: 10.1140/epjc/s10052-020-8192-3.
- [116] Antonio Pich. QCD-Duality Approach to Nonleptonic Weak Transitions: Towards an Understanding of the $\Delta I = 1/2$ Rule. *Nucl. Phys. B Proc. Suppl.*, 7:194, 1989. doi: 10.1016/0920-5632(89)90569-0.
- [117] Matthias Jamin and Antonio Pich. QCD corrections to inclusive $\Delta S = 1, 2$ transitions at the next-to-leading order. *Nucl. Phys. B*, 425:15–38, 1994. doi: 10.1016/0550-3213(94)90171-6.
- [118] Antonio Pich and Eduardo de Rafael. Bounds on the Strength of $\Delta I = 1/2$ Weak Amplitudes. *Phys. Lett. B*, 189:369–374, 1987. doi: 10.1016/0370-2693(87)91449-3.
- [119] S. Aoki et al. FLAG Review 2019: Flavour Lattice Averaging Group (FLAG). *Eur. Phys. J. C*, 80(2):113, 2020. doi: 10.1140/epjc/s10052-019-7354-7.
- [120] Vincenzo Cirigliano, Adam Falkowski, Martín González-Alonso, and Antonio Rodríguez-Sánchez. Hadronic τ Decays as New Physics Probes in the LHC Era. *Phys. Rev. Lett.*, 122(22):221801, 2019. doi: 10.1103/PhysRevLett.122.221801.